Journal of Science & Technology in the Tropics

Volume 9 Number 1 June 2013

JOSTT

DEDICATED TO THE ADVANCEMENT OF SCIENCE AND TECHNOLOGY RELATED TO THE TROPICS

Journal of Science & Technology in the Tropics

Volume 9 Number 1 June 2013

Volume 9 Number 1
June 2013

ISSN 1823-5034

AKADEMI SAINS MALAYSIA

COSTAM

Journal of
Science &
Technology
in the Tropics
Volume 9 Number 1 June 2013

CONTENTS

INSTRUCTIONS TO CONTRIBUTORS

JOSTT is a multi-disciplinary journal. It publishes original research articles and reviews on all aspects of science and technology relating to the tropics. All manuscripts are reviewed by at least two referees, and the editorial decision is based on their evaluations.

Manuscripts are considered on the understanding that their contents have not been previously published, and they are not being considered for publication elsewhere. The authors are presumed to have obtained approval from the responsible authorities, and agreement from all parties involved, for the work to be published.

Submission of a manuscript to JOSTT carries with it the assignment of rights to publish the work. Upon publication, the Publishers (COSTAM and ASM) retain the copyright of the paper.

Manuscript preparation

Manuscripts must be in English, normally not exceeding 3500 words. Type double spaced, using MS Word, on one side only of A4 size with at least 2.5 cm margins all round. Number the pages consecutively and arrange the items in the following order: title page, abstract, key words, text, acknowledgements, references, tables, figure legends.

Title page

Include (i) title, (ii) names, affiliations and addresses of all authors, (iii) running title not exceeding five words, and (iv) email of corresponding author.

Abstract and key words

The abstract, not more than 250 words, should be concise and informative of the contents and conclusions of the work. A list of not more than five key words must immediately follow the abstract.

Text

Original research articles should be organized as follows: Introduction, Materials and Methods, Results, Discussion, Acknowledgement, References. The International System of Units (SI) should be used. Scientific names and mathematical parameters should be in italics.

References

References should be cited in the text as numbers enclosed with square [ ] brackets. The use of names in the text is discouraged. In the reference section, the following examples should be followed:

1. Yong H.S., Dhaliwal S.S. and Teh K.L. (1989) A female Norway rat, *Rattus norvegicus,* with XO sex chromosome constitution. *Naturwissenschaften* **76**: 387-388.
2. Beveridge W.I.B. (1961) *The Art of Scientific Investigation*. Mercury Book, London.
3. Berryman A.A. (1987) The theory and classification of outbreaks. In Barbosa P. and Schultz J.C. (eds.) *Insect outbreaks* pp. 3-30. Academic Press, San Diego.

Tables

Tables should be typed on separate sheets with short, informative captions, double spacing, numbered consecutively with Arabic numerals, and do not contain any vertical lines. A table should be set up to fit into the text area of at most the entire page of the Journal.

Illustrations

Black-and-white figures (line drawings, graphs and photographs) must be suitable for high-quality reproduction. They must be no bigger than the printed page, kept to a minimum, and numbered consecutively with Arabic numerals. Legends to figures must be typed on a separate sheet. Colour illustrations can only be included at the author's expense.

Proofs and reprints

Authors will receive proofs of their papers before publication. Order for reprints must be made when returning the proofs.

Submission

Manuscripts (including all figures but not original artwork), should be submitted to:

The Editorial Office
Journal of Science and Technology
in the Tropics
Academy of Sciences Malaysia
902-4 Jalan Tun Ismail
50480 Kuala Lumpur, Malaysia

E-mail: jostt@akademisains.gov.my

JOSTT is listed in Scopus

EDITORIAL

United Nations International Year of Water Cooperation

In December 2010, the United Nations General Assembly declared 2013 as the United Nations International Year of Water Cooperation (Resolution A/RES/65/154). While Malaysia is blessed that it does not have a common border with another country where a river marks a border, except maybe Brunei, many countries have this problem. Countries in Asia, Africa, South America, North America and Europe face this problem.

In reflection of this declaration, the 2013 World Water Day on 22 March 2013, also will be dedicated to water cooperation. Therefore, UN-Water has called upon UNESCO to lead the 2013 United Nations International Year on Water Cooperation, in particular because of the Organization's unique multidisciplinary approach which blends the natural and social sciences, education, culture and communication. Given the intrinsic nature of water as a transversal and universal element, the United Nations International Year on Water Cooperation naturally would embrace and touch upon all these aspects.

The objective of this International Year is to raise awareness, both on the potential for increased cooperation, and on the challenges facing water management in light of the increase in demand for water access, allocation and services. The Year will highlight the history of successful water cooperation initiatives, as well as identify burning issues on water education, water diplomacy, transboundary water management, financing cooperation, national/international legal frameworks, and the linkages with the Millennium Development Goals. It also will provide an opportunity to capitalize on the momentum created at the United Nations Conference on Sustainable Development (Rio+20), and to support the formulation of new objectives that will contribute towards developing water resources that are truly sustainable.

Celebrations throughout the Year will include featured events at UNESCO Headquarters in Paris, as well as many other events organized by various stakeholders around the world. Such events will seek to promote actions at all levels in relevant areas including education, culture, gender, the sciences, conflict prevention and resolution, as well as ethics, among others.

While we in Malaysia is not involved in transboundary issues, it is appropriate that we as a nation be more concerned with water conservation, both at the domestic, agriculture and industrial sectors. Management of water is a very important issue that Malaysia should address.

Dr Salleh Mohd. Nor and Dr Ong Eng Long
Co-Chairman, JOSTT

Journal of Science and Technology in the Tropics (2013) 9: 5-14

Redescription of *Armigeres* (*Leicesteria*) *longipalpis* (Leicester) (Diptera: Culicidae) from Sarawak, Malaysia

Takako Toma[1], Ichiro Miyagi[1, 2], Takao Okazawa[3], Yukiko Higa[4], Siew Fui Wong[5], Moi Ung Leh[5] and Hoi Sen Yong[6]

[1]Laboratory of Medical Zoology, School of Health Sciences, Faculty of Medicine, University of the Ryukyus, Nishihara, Okinawa, 903-0215 Japan
[2]Laboratory of Mosquito Systematics of Southeast Asia and Pacific, c/o Ocean Health Corporation, 4-21-11, Iso, Urasoe, Okinawa, 901-2132 Japan
[3]International Student Center, Kanazawa University, Kakuma, Kanazawa, Ishikawa, 920-1192 Japan
[4]Department of Vector Ecology and Environment, Institute of Tropical Medicine (NEKKEN), Nagasaki University. Sakamoto 1-12-4, Nagasaki, 852-8523 Japan
[5]Sarawak Museum Department, 93566 Kuching, Sarawak, Malaysia
[6]Institute of Biological Sciences, University of Malaya, 5603 Kuala Lumpur, Malaysia
(*coresponding author e-mail: topmiyagii@ybb.ne.jp)

Received 14-01-2013; accepted 04-02-2013

Abstract Redescription of *Armigeres* (*Leicesteria*) *longipalpis* (Leicester) was presented based on the specimens collected in Sarawak, Malaysia. Illustrations of abdominal ornamentations of adult male and female, pupa and larva were given for the first time. The larvae of the species were collected in water accumulation of green bamboo stumps and splits, and tree holes in mountain forest.

Keywords *Armigeres longipalpis* – redescription – immature stages – Sarawak – Malaysia

INTRODUCTION

During a recent mosquito survey in Sarawak, a fairly large series of adult and larval specimens and associated larval and pupal exuviae of the species belonging to the subgenus *Leicesteria* of genus *Armigeres* were collected and available for description [1, 2]. Some of them are identified as *Armigeres* (*Leicesteria*) *longipalpis* (Leicester), 1904 based on the male genitalia [3]. This species was originally described from Kuala Lumpur, Malaysia and then confused with *Armigeres* (*Leicesteria*) *cingulatus* (Leicester), 1908 from the same type locality, due to the resemblance and variability of the pale bands on the abdomen. The taxonomic confusion between the species was clarified by Barraud [4], Macdonald [3] and Thurman [5]. The structures of the male genitalia are useful in distinguishing these species. With existing descriptions of adult male and female of *Ar. longipalpis* [3 – 5], the important adult characters and male genitalia are given briefly by current standards. Illustrations of pupa, larva and abdominal

ornamentations of male and female of this species are also given for the first time in this paper.

MATERIALS AND METHODS

Specimens of *Armigeres longipalpis* were collected as larva from green bamboo stumps by I. Miyagi, T. Okazawa and T. Toma: 5 ♂♂ on pin with pupal (P) and/or larval (L) exuviae mounted on slide (274, 275, 296, 446, 409) and genitalia (G) on slide (143, 154, 135, 126, 142), 3♂♂ with P, L (227, 285, 297), 5♀♀ with P, L (155, 167, 201, 202, 428), 3♀♀, 6 whole larvae on slides collected at Ba'Kelalan and Bario (3° 59' 0" N, 115° 37' 0" E) Kelabit highland (ca 1,000 m elevation), on 21 – 30 August 2008. 1♂ with P, L (478) and G (161), 2♂♂ with P, L (423, 472); 1♀ with P, L (495) at Matang National Park, Kuching on 5 September 2008.

The illustrations of the abdominal ornamentation in the species were based mainly on fresh specimens, as deformity in the colorations of the sterna occurs in dry specimens [6]. The terminology used for the adults and immature stages mainly follows Harbach and Knight [7, 8]. The siphon and trumpet indices of larva and pupa used here follow Belkin's [9] "Ratio of dorsal length to median width". The specimens examined are deposited in the Sarawak Museum, Kuching, Malaysia.

DESCRIPTIONS AND DISCUSSION

***Armigeres* (*Leicesteria*) *longipalpis* (Leicester)**
(Figs 1, 2, 3 and Tables 1, 2)
Leicesteria longipalpis Leicester in Theobald, 1904, *Entomologist*, 37: 211.
Armigeres (*Leicesteria*) *longipalpis*. Macdonald, 1960, *Stud. Inst. Med. Res. Malaya*, 29: 126 (♀, ♂, L).

Description
Female (Fig. 1A, C, D, H) – *Head*: Vertex covered with flat, broad, dark scales and with a central patch of pale broad scales; occiput with a posterior patch of several pale and brown upright forked scales; inter-ocular with one dull yellow seta and white scales; ocular line with 6 well developed reclinate dark setae and with white scale line; postgena (in lateral view) dark, divided by pale horizontal scale patch. Proboscis, ca 2.3 mm, uniformly dark dorsally without ventral pale scale line. Maxillary palpus ca 1.0 mm, dark without pale scales. Clypeus with several pale scales on outer surface. Pedicel yellowish, inner surface with a patch of white scales mingled with dark scales. Anntena ca 2.0 mm long, first segment of flagellomere with pale scales. *Thorax*: Integument dark brown with narrow, curved, light brown and golden scales; antealar area, from lateral scutal fossal to

wing root, with a line of white broad and narrow scale patch; median prescutellar area with several white scales (sometimes replaced with light brown scales) and two strong prescutellar setae. All lobes of scutellum with a patch of dull yellow broad scales and with 3 or 4 well developed marginal setae. Antepronotal lobe covered closely with white broad scales and with 8 well developed dark setae; postpronotal lobe with grayish broad scales and 7 or 8 dark setae above and with white broad scales below. Paratergite with several pale setae. Pleuron of upper proepisternal, subspiracular and postspiracular areas, mesokatepisternum and mesanepimeron with patch of white scales; approximately 10 long dull yellow setae on mesokatepisternum and 15 dark setae on upper mesepimeral area. *Legs*: All coxae with patches of white and dark scales and with yellowish setae on anterior side; all legs dark dorsally with white scale line from base to apex ventrally, and with a row of several conspicuous spine-like setae, without pale rings. Forefemur,

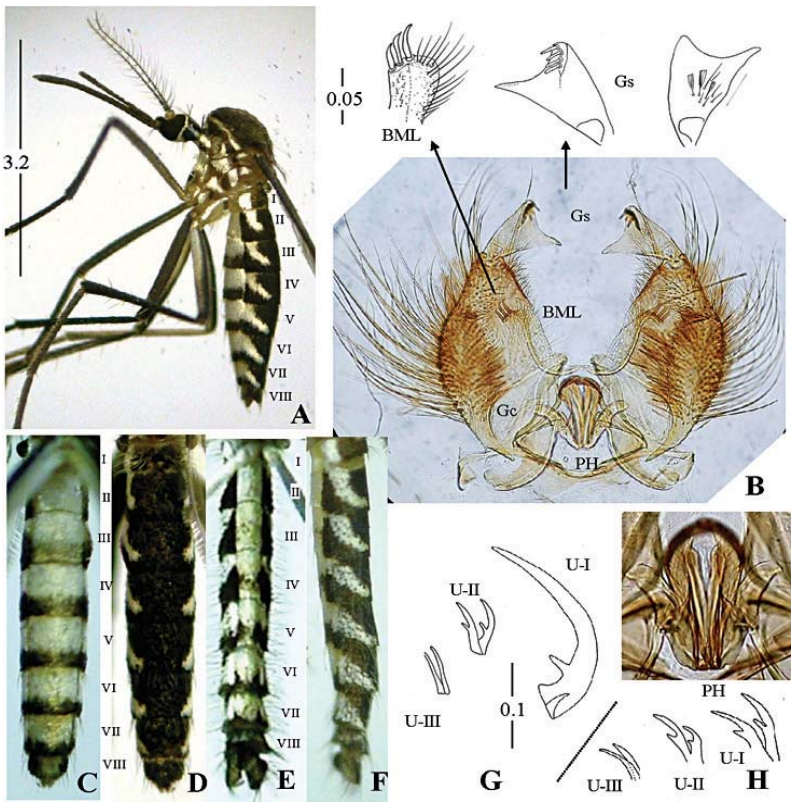

Figure 1. Adult female (A, C, D, H) and male (B, E, F, G) of *Armigeres* (*Leicesteria*) *longipalpis*. A, whole body (lateral aspect); B, genitalia (ventral aspect); C, E, abdominal sterna I – VIII (ventral aspect); D, abdominal terga I – VIII (dorsal aspect); F, abdominal terga I – VIII (lateral aspect); G, H, ungues I – III. BML, basal mesal lobe; Gc, gonocoxite; Gs gonostylus (both aspects); PH, phallosome; U-I, U-II and U-III, fore-, mid- and hindungues. Scales: mm.

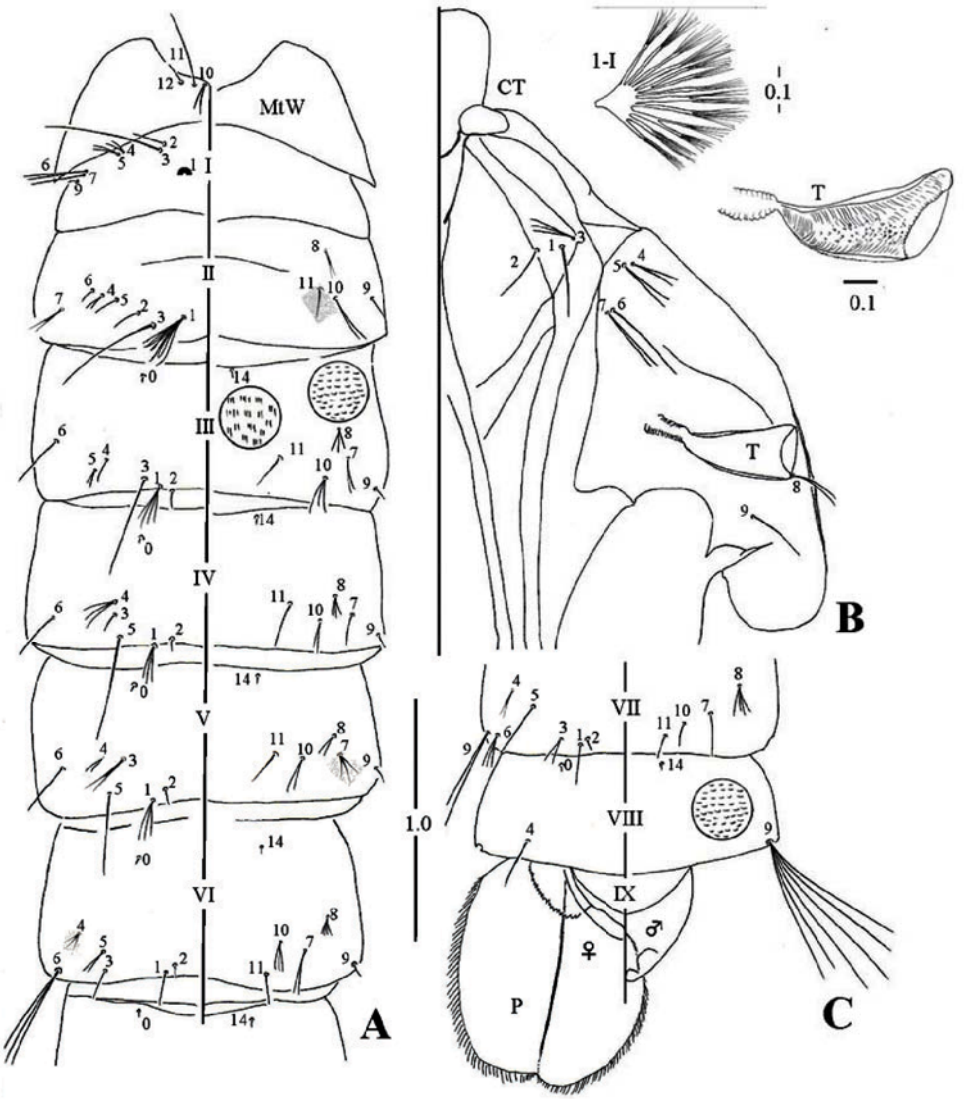

Figure 2. Pupa (exuvia) of *Armigeres* (*Leicesteria*) *longipalpis*. A, metathoracic wing (MtW) and abdominal segments I – VI (both aspects); B, part of cephalothorax (CT); C, abdominal segments VII – IX and paddle (P) (lateral aspect). 1-I, seta 1 on abdominal segment I; T, trumpet. Scales: mm.

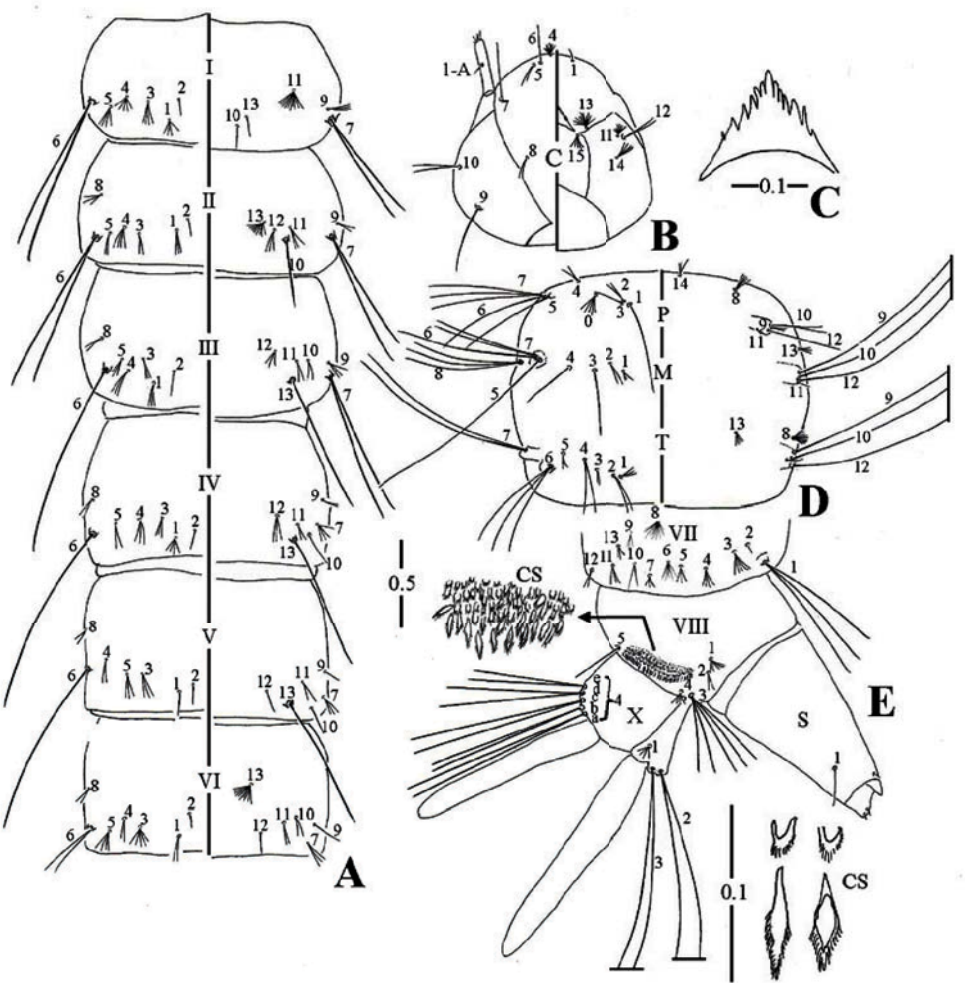

Figure 3. Fourth-instar larva of *Armigeres* (*Leicesteria*) *longipalpis*. A, abdominal segments I – VI (both aspects); B, head (both aspects); C, dorsomentum (ventral aspect); D, thorax (both aspects); E, abdominal segments VII, VIII, X and siphon (S) (lateral aspect). CS, comb scales. Scales: mm.

ca 2.50 mm, foretibia 2.25 mm, foretarsus I 1.35 mm, II 0.75 mm, III 0.5 mm, IV 0.32 mm, V 0.27 mm. All ungues as in Fig. 1H; foreungues (U-I) and midungues (U-II) with submedian teeth; hindungues (U-III) small, simple. *Wing*: Length ca 3.50 mm. Cell R_2 ca 1.5 times the length of its stem; alula with a row of small scales; upper calypter with a row of hair-like scales; halter, capitellum dark, scabellum light in colour. *Abdomen*: Length ca 3.50 mm; sterna (Fig. 1C), I, II white to light yellow; III – VII white basally with black apical band, VIII mostly white scaled; terga (Fig. 1D), I blackish with many yellowish setae dorsolaterally; lateral white markings on terga II – VII curved obliquely to the dorsum, forming dorsal subapical pale band on each segment, the pale band usually interrupted dorsally without lateral yellow brown scales (Fig. 1A, D).

Male (Fig. 1B, E, F, G) – Resembles the female except in the following characters. *Head*: Proboscis, ca 2.50 mm with a line of dull pale scale on underside reaching from base to near tip. Palpus dark, ca 2.1 mm, little longer than proboscis, 1st segment as long as 2nd segment, junction of the segments white faintly; 2nd and 3rd with 2 or 3 well developed setae. Antenna little shorter than proboscis and maxillary paplus. *Thorax*: Pleural patches more conspicuous than those of female. *Abdomen*: Ornamentation as in female but with many pale and dark setae on lateral and dorsal parts of all segments (Fig. 1E, F). *Legs*: Foretarsus IV apparently shorter than V. Foreungues (U-I) large, unequal in size, the larger one with submedian small tooth, the other very small, obsolete; midungues small (U-II), equal, both with small submedian tooth; hindungues (U-III) smallest, equal in size, without submedian tooth (Fig. 1G). *Wing*: Length ca 3.6 mm. *Genitalia* (Fig. 1B): Tergum IX with apical area partly sclerotized and divided into two lobes by a shallow U shaped depression with 7 – 10 fine setae on each lobe. Sternum IX broad with many scales entirely and with 20 – 25 fine setae on apical margin. Gonocoxite (Gc): broad, tapering at base, 1.57 as long as its breadth at center, with dense longitudinal patch of scales ventrally and with many long setae laterally. Basal mesal lobe (BML): finger-like with a row of 3 graded blunt spines on outer apical margin and with many fine setae on inner lateral margin. Gonostylus (Gs): triangular in shape with 3 or 4 spines on dorsal corner and with few small scales and setae on central surface. Phallosome (PH) oval in shape, with crenulated apical margin.

Pupa (Fig. 2, Table 1) – *Cephalothorax* (Fig. 2B): Yellow to light brown pigmentation. Trumpet (T), 0.45 mm, index ca 2.5. Setae 1-CT single longer than others. *Abdomen*: Length ca 5.0 mm; very fine imbricative spicules laterally on segments II – VIII and very fine needle-like spicules on segements II – IV ventrocentrally (Fig. 2A, C); seta1-I long, fanlike with 8 – 13 main branches; 1-II conspicuous with 7 – 30 branches; 3-II, III and 5-IV, V long, single; seta 6-VI long

Table 1. Numbers of branches for pupae of *Ar. longipalpis* (Leicester).

Seta No	Cephalo-thorax	Abdominal segments							
		I	II	III	IV	V	VI	VII	VIII
0	-	-	-	1	1	1	1	1	1
1	1	M+	7–30	4–8	3–8	3–5	1–5	1, 2	-
2	1, 2	1	1	1	1	1	1	1	-
3	3–5	1	1*	1*	1–3	2–7	1, 2	1–3	-
4	2–4	2–5	1–6	1–3	3–7	2–5	2, 3	1, 2	1, 2
5	1–4	1, 2	1–6	1–3	1*	1*	1–4*	1, 2	-
6	1	1–3	1–6	1–4	1–4	1–3	1–3	2–4	-
7	1–3	1–5	2–5	1–7	1–5	3–5	1–5	1–3	-
8	2–4	-	2	2–4	2–5	2–4	2–4	2–6	-
9	1	1, 2	1	1	1	1	1	2–6*	6–9*
10	2–4	-	1–4	1–3	1, 2	1, 2	1–3	1, 2	-
11	1	-	1	1	1	1	1	1–5	-
12	1, 2	-	-	-	-	-	-	-	-
14	-	-	-	1	1	1	1	1	1

+ dendritic with many branches. *long, weakly aciculated
Obsolete and missing setae are shown with a hyphen (-).
Specimens examined: 4 pupal exuviae from Bario and Bakelalan, Sarawak.

Table 2. Numbers of branches for fourth-instar larvae of *Ar. longipalpis* (Leicester).

Seta No	Head	Thorax			Abdominal segments							
		P	M	T	I	II	III	IV	V	VI	VII	VIII
0	-	5-7	-	-	-	-	-	-	-	-	-	-
1	1	1	3–5	2–6	2–6	2–5	4–6	3–6	2	2	2, 3*	5–20
2	-	2, 3	1–3	2, 3	1, 2	1	1, 2	1, 2	1	1	1	1–4
3	-	1–3	1, 2	2–4	3–7	2–4	2–4	2–4	3–9	2	4–6	3–8*
4	8–16	2–4	1, 2	2, 3	4–13	4–12	2–4	2–4	2	3	2–5	2–4
5	2	1*	1*	1–3	3–5	1–4	2–4	2, 3	3–5	2–6	3–6	1*
6	1	1*	1, 2*	2–5*	2–5*	2*	1*	1, 2*	1, 2*	2, 2*	5–10	-
7	1, 2	3–8	2–4*	2–5*	2–4*	1, 2*	1, 2*	4–7	3–7	3–7	3–9	1-X=4–8
8	1–3	3–8*	2, 3	10–20	-	3-6	2, 3	2, 3	2–4	2–5	11–15	
9	1	1–3	1, 2*	1*	3, 4	2–4	1–5	2–4	1–4	1–5	4–12	2-X=2*
10	1–3	1, 2	1, 2*	1*	1, 2	1, 2	2–4	1–4	2, 3	2–4	2, 3	
11	7, 8	1	1, 2	1	10–14	3–6	2–4	2–4	2–4	2–5	6–13	3-X=1, 2*
12	2–5	1	1, 2*	1, 2*	-	2–6	2–4	2–4	1–3	1, 2	2–4	
13	10–18	-	11–21	6–10	1, 2	10–14	1	1*	1*	9–16	10–18	4-X=10,11*
14	5–7	2–4	-	-	-	-	-	-	-	-	-	-
15	5–9	-	-	-	-	-	-	-	-	-	-	-

*long, weakly aciculated.
Obsolete and missing setae are shown with a hyphen (-).
Specimens examined: 5 fourth-stage larvae from Bario and Bakelalan, Sarawak.

with 1 – 3 branches; 9-VII long with 2 – 6 aciculate branches, 9-VIII long with 6 – 9 aciculate branches. *Paddle* (P): Length ca 0.95 mm, lightly pigmented except at base, with midrib from base to apex and with marginal filamentous spicules; seta 1-P usually obsolete, if present single, very fine. *Genital lobe*: Extending to ca 0.47 of paddle in male, to ca 0.29 of paddle in female.

Fourth-instar larva (Fig. 3, Table 2) – *Head* (Fig. 3B): Ca 1.13 mm, slightly shorter than the width; light yellow-brown in colour; dorsomentum (Fig. 3C) with a strong median tooth and with 6 or 7 teeth on each side. Seta 1-C small, single, tapering; 9-C long, single, stronger than the others. *Antenna*: Integument smooth, yellow in colour, length ca 0.27 of head; shaft about the same breadth from base to apex, seta 1-A single at 0.5 from base. *Thorax* (Fig. 3D): Seta 1-P long, single; 3-M single or double, shorter than 1-P; 5-M long, single; 8-M long, 2, 3 branched; 9, 10, 12-M long, single or double; 7-T long, 2 – 5 branched; 9, 10-T long, single. All these setae more or less aciculated. *Abdomen* (Fig. 3 A, E): All segments without ventral patch of fine spicules. Setae 1-I weak with 2 – 6 branches; 6-I, II large, usually double; 6-III large, single; 6-IV large, single or double; 7-I long, 2 – 4 branched; 7-II large, single or double; 13-III – V large, single; 1-VII large, 2 or 3 branched; 3-VIII well developed with 3 – 8 branches. All these large setae more or less aciculated and arising from small lightly sclerotized plates or tubercles. Comb (CS) of 70 – 80 fringed scales including 2 types, the distal scales larger with central sharp-pointed spine and the basal scales smaller rounded with uniform fringes. Saddle incomplete, pigmented brown; anal papilla long-oval with rounded apices. Siphon: Length variable, 0.89 – 0.97 mm, index 1.4 – 1.5; seta 1-S usually single or double, arising about 0.20 from apical end.

TAXONOMIC DISCUSSION

Although the subgenera *Armigeres* and *Leicesteria* of the genus *Armigeres* are easily distinguished in the adult stages, reliable separations of the pupal and larval stages are not known [3, 10].

Armigeres longipalpis is characterized as follows: In adult, thorax is not strongly produced over head in lateral view; clypeus has several pale scales; lateral white markings on terga II – VII curved to the dorsum but do not join to form complete bands without additional distinct lateral yellow brown scales; all legs are dark without pale rings; foretarsus IV is apparently shorter than V in male. Male genitalia is unique in conical gonocoxite with dense patch of scales and setae; in triangular gonostylus with 3 or 4 dorsoapical spines and with few fine scales and setae on central part; basal mesal lobe has a row of 3 graded spines and many marginal setae on apical margin. In general appearance, the female of *Ar. longipalpis* somewhat resembles *Armigeres* (*Leicesteria*) *digitatus* (Edwards), but

its clypeus is bare and palpus is 2/3 length of proboscis [3, 5]. The larva and pupa of this species are very similar to those of *Armigeres* (*Leicesteria*) *annulipalpis* (Theobald) [2]. The larva differs in the shapes of comb scales and number of branches in setae 6, 7-II, III and abdominal seta 5-VIII. There are no reliable distinguishing characters for the pupal stage.

Biological notes

The larvae of *Ar. longipalpis* were found in green living bamboo stumps and splits in bamboo forest in Bario, Ba'Kelalan, Matang National Park, Sarawak. Nothing is known of the biting habits.

Distribution

Malaysia (Selangor and Sarawak), Indonesia, Thailand, Cambodia, Laos, Vietnam, India.

Acknowledgements – We thank the Sarawak Forestry Department for granting permission for sampling of two-winged flies (Diptera) in the Bario highland and Matang National Park, Sarawak.

REFERENCES

1. Miyagi I. and Toma T. (2009) Culicidae and Corethrellidae (Diptera) collected in Sarawak, Malaysia from 2005 – 2008. *Sarawak Museum Journal* **66** (87): 313–331.
2. Toma T., Miyagi I., Okazawa T., Higa Y., Wong S.F. and Yong H.S. (2012) Redescriptions of *Armigeres annulipalpis* and *Armigeres flavus* (Diptera: Culicidae) from Sarawak, Malaysia. *Journal Science and Technology in the Tropics* **8:** 5–19.
3. Macdonald W.W. (1960) On the systematics and ecology of *Armigeres* subgenus *Leicesteria* (Diptera; Culicidae). *Studies from the Institute for Medical Research Federated Malay States* **29:** 110–159.
4. Barraud P.J. (1934) *The fauna of British India, including Ceylon and Buruma. Diptera, Culicidae. Tribes Magarhinini and Culicini*. Vol. 5, 463 pp., 106 figs., 7 pls.
5. Thurman E.B. (1959) *A Contribution to a Revision of the Culicidae of Northern Thailand*. Bull. A-100, 182 pp., University of Maryland Agriculture Experiment Station, Maryland.
6. Toma T., Miyagi I., Okazawa T., Higa Y. and Leh C. (2010) Redescriptions of five species of the genus *Armigeres*, subgenus *Armigeres* (Diptera: Culicidae) collected from fallen coconut fruits at the coastal plains of Sarawak, East Malaysia. *Medical Entomology and Zoology* **3:** 281–308.
7. Harbach R.E. and Knight K.L. (1980) *Taxonomists' Glossary of Mosquito Anatomy*. Plexus Publishing Inc., Marlton.
8. Harbach R.E. and Knight K.L. (1981) Corrections and additions to taxonomists' glossary of mosquito anatomy. *Mosquito Systematics* **13:** 201–217.

9. Belkin J.N. (1962) *The Mosquitoes of the South Pacific (Diptera)*. Vols. 1 and II. University of California Press, Barkeley and Los Angeles.
10. Steffan W.A. (1968) *Armigeres* of the Papuan subregion (Diptera: Culicidae). *Journal of Medical Entomology* **5:** 135–159.

Journal of Science and Technology in the Tropics (2013) 9: 15-23

Effect of contrasting soil textures on the nutritional status of three latex timber clones (*Hevea brasiliensis*)

Shafar Jefri Mokhatar, Noordin Wan Daud* and Noorsuhaila Abu Bakar
Department of Crop Science, Faculty of Agriculture, Universiti Putra Malaysia,
43400 Serdang, Selangor, Malaysia
(Corresponding author email: wnordin@agri.upm.edu.my)

Received 01-03-2013; accepted 22-03-2013

Abstract The main source for natural rubber is the rubber tree. *Hevea brasiliensis* or rubber has been planted on marginal soils due to competition for land from other crops and from property development. In Malaysia, marginal soils can comprise Oxisols, Ultisols and Inceptisols. The objective of this study was to assess the nutrient uptake of rubber plants in relation to contrasting soil textures. Three latex timber clones were used in this study, *viz*. RRIM 2001, RRIM 2025 and RRIM 3001. The soils were from the Munchong and Holyrood series. Several physical and chemical properties of the soils were analyzed prior to the study. Compound fertilizers (10.7 N: 16.6 P: 9.5 K: 2.4 Mg) were applied at the current recommended rate, i.e. 18.75 kg/ha. After a year the nutritional status of the matured leaves was analyzed. Results show that the texture of the soil influenced the chemical properties of the soil. The sandy soil of the Holyrood series had a lower CEC than the clayey soil of the Munchong series, and was able to retain much less of the nutrients applied as fertilizer to be available for plant uptake. From the leaf nutrient analyses, it would appear that rubber plants grown in the Holyrood series had significantly lower nutrient values, and were more likely to show visual nutrient deficiency symptoms compared with plants grown in the Munchong series soil. It may be concluded that a clayey soil, such as the Munchong series, is much better than a sandy soil, like the Holyrood series, in providing nutrients for plant uptake. Of the three clones used, RRIM 3001 showed similar nutrient status when grown in the clayey soil as the other two clones except for nitrogen content. However, it had lower nutrient contents than RRIM 2001 and RRIM 2025 in the sandy soil; hence, it may be concluded that this clone requires more applied nutrients in order to achieve optimum growth. The results also suggest that there should be specifically different agronomic practices when planting rubber in soils with contrasting textures.

Keywords rubber – latex timber clones – nutrition – Inceptisol – Oxisol

INTRODUCTION

Hevea brasiliensis or the rubber tree is the main source of natural rubber. Southeast Asia has been the main producer of natural rubber because of its climate suitability and absence of devastating diseases such as South American Leaf Blight (SALB).

Demand for natural rubber increased tremendously with the development of the automotive industry in several countries, and the increase in crude oil prices which has a direct impact on the cost of producing synthetic rubber. Synthetic rubber is synthesised from petroleum byproducts. Currently, about two-third of the total rubber are synthetic rubber, and some manufacturers look for natural rubber for replacing synthetic rubber due to crude oil prices [1].

Due to land limitation in Malaysia, property development and the cultivation of other crops (mainly, oil palm), competition for land use is very high. Hence, rubber cultivation had to be shifted to more marginal land [2, 3]. In order to optimize production, new clones of rubber have been produced extensively by the Malaysian Rubber Board. RRIM 2001, RRIM 2025 and RRIM 3001 are classified as Latex Timber clones, which can produce both high yields of latex and timber.

Clones are a group of plants which are genetically identical and are derived from a single parent. For vegetatively propagated plants like *H. brasiliensis*, clones are normally mass-propagated by bud-grafting. It is important to assess the adaptability of new rubber clones to soils commonly used for rubber cultivation (e.g. Munchong series) as well as to marginal soils (such as Holyrood series) in order to establish proper agronomic management practices.

According to USDA soil taxonomy, the Munchong series has been classified as a very fine kaolinitic, isohyperthermic Tropeptic Haplorthox [2, 4, 5]. The Munchong series soil ranges from a silty clay loam to silty clay which is yellowish brown to strong brown. This soil has been classified as a first class soil for rubber planting in terms of soil-crop suitability [2, 6]. The Holyrood series has been classified as a fine loamy, siliceous, isohyperthermic Oxic Dystropept. The Holyrood series soil ranges from a sandy loam to a sandy clay loam which is yellowish brown to brownish yellow. This soil has been classified as a fourth class soil for rubber planting in terms of soil-crop suitability [2, 4, 6].

A nursery trial was carried out to assess the performance of three new latex timber clones, *viz.* RRIM 2001, RRIM 2025 and RRIM 3001, grown in soils with two types of texture, i.e. clayey and sandy soils. Information on their growth performance has also been reported elsewhere [7, 8]. This paper discusses the response of the three clones in terms of their nutritional status in relation to the contrasting soil textures.

MATERIALS AND METHODS

Three new latex timber clones, RRIM 2001, RRIM 2025 and RRIM 3001, at three months age obtained from Malaysian Rubber Board were used in the study. The soils in which the clones were grown were from the Munchong and Holyrood series. Soil was collected from top soil and sub-soil, 0-45 cm depth.

Soil profile was described in order to ensure the type of soil used. The plants were grown in soil-filled polythene bags measuring 45.72 cm x 50.8 cm.

The experimental setup was a factorial randomized complete block design (RCBD) with four blocks. Before the study began, several physical and chemical properties of the soils were analyzed to assess their fertility status. Particle size distribution was determined by the pipette method [9]. Total carbon was measured by the combustion technique [10], using a CR-412 carbon analyzer (LECO Corporation, St. Joseph, USA). Total nitrogen was determined using the modified Kjeldahl method [11]. Soil exchangeable bases (K, Mg) and cation exchange capacity (CEC) were determined by using the 1M NH_4OAc (pH 7.0) method [12]. Adsorbed NH_4^+ was displaced with potassium sulphate solution and determined using an auto-analyzer (Quickchem, FIA 8000, Lachat Instruments, and USA).

Compound fertilizers (10.7 N: 16.6 P: 9.5 K: 2.4 Mg) were applied at the current recommended rate of 18.75 kg/ha. After one year's growth, the leaf nutritional status (N, P, K and Mg) was analyzed. Leaf sampling was done according to the method adopted by the Malaysian Rubber Board: four basal leaves from the first sub-terminal whorl were collected as a leaf sample [13]. The sampled leaves (leaf and petioles) were separated from the stems and placed in a forced draft oven and dried at 60ºC for 48 hours. After that, the weights were determined using a weighing balance.

The leaf concentrations of nitrogen (N), phosphorus (P) and potassium (K) in the finely ground dried leaves were determined. Samples weighing 0.25 g were each digested in 5 mL of concentrated sulphuric acid (H_2SO_4) on a hot plate at 450°C in a fume chamber for 7 minutes. Ten mL of hydrogen peroxide (H_2O_2) was then added into the mixture, and heating was continued for another four minutes. The solution was made up to 100 mL with distilled water and filtered with filter paper no. 5.

The contents of N and P were determined using an auto-analyzer (Lachat Instruments, Model Quickhem IC + FIA 8000 Series) while K and Mg contents were measured using an atomic absorption spectrophotometer (Perkin Elmer, Model AAS 3110). Analysis of Variance (ANOVA) was performed on the data obtained using the software SAS 9.1 (SAS Institute, Inc. Cary NC. USA). The Least Significant Difference (LSD) test at $P<0.05$ was employed for comparison of means only if F values were significant.

RESULTS AND DISCUSSION

Soil physical-chemical properties

The Munchong series soil which is derived from shale, a sedimentary rock, is yellowish brown to strong brown in colour. As it is a highly weathered soil,

the particle size distribution was dominantly clay (62.79%), followed by sand and silt (Table 1). The Holyrood series soil is derived from sub-recent riverine alluvium, and is yellowish brown to brownish yellow in colour. As a younger soil, this soil was dominant in sand (67.57%), followed by clay and silt. The cation exchange capacity (CEC) of the soils was generally low, with values of 8.1 and 4.7 $cmol_{+}kg^{-1}$ for the Munchong and Holyrood series, respectively. These CEC_{NH4OAc} values indicate that the soils' ability to retain cations was quite limited. Their pH values of 4.20 and 4.40, respectively, were acidic. As the Holyrood series is new soil (Inceptisol), total carbon and nitrogen were very low. Due to its attribute, of being sandy, quite limited vegetation grows naturally on it, which explains the results of low carbon and nitrogen contents [2, 14]. Soil-available phosphorus and the exchangeable bases, K and Mg, were also low. It is well-known that in the tropical regions, Oxisol is inherently low in P and show high P fixation. Due to its clay mineralogy which is dominated by kaolinite and gibbsite, phosphate fertilizer applied to Oxisols is usually locked up by the iron oxides [2, 15, 16]. The Munchong series is a soil developed from the sedimentary rock, shale, and is highly weathered, resulting in the low content of K [17]. Potassium is usually lacking in highly weathered soils, such as an Oxisol, because it is easily leached out into the groundwater [3, 16].

Leaf nutrient content

Data from the leaf nutrient analyses show that the rubber plants grown in the Holyrood series soil generally had significantly lower contents of leaf nutrients compared with the plants grown in the Munchong series soil (Table 2). Clone RRIM 3001 grown in Holyrood series soil showed significantly lower K content compared with RRIM 2001 and RRIM 2025 (Table 3). It also had a significantly lower N content compared with RRIM 2025 and a lower Mg content compared with RRIM 2001.

Due to the sandy texture of the soil (Holyrood series), nutrients would be more easily leached out and volatized which would have resulted in less nutrients remaining for plant uptake. Leaching of nutrients and a limited or low capacity of the soil to retain nutrients result from the properties of the soil such as low

Table 1. Selected physical and chemical properties of the test soils (*n*=4).

Soil Series	pH	CEC (cmol -kg^{-1})	Particle size			Total C	Total N	Total P	Exch. K	Exch. Mg
			Clay (%)	Silt (%)	Sand (%)	(%)	(%)	mg kg^{-1}	$Cmol_c\ kg^{-1}$	
Munchong	4.20	8.1	62.79	10.89	26.21	1.6	0.13	250	0.9	1.6
Holyrood	4.40	4.7	22.39	9.93	67.57	0.4	0.09	300	0.7	0.9

Table 2. Leaf nutrient contents after one year's growth (comparing the effect of soil series on each clone).

Soil	N (%)			P (%)			K (%)			Mg (%)		
series*	C1**	C2**	C3**	C1	C2	C3	C1	C2	C3	C1	C2	C3
M	2.52a	2.80a	2.85a	0.17a	0.17a	0.19a	0.78a	0.83a	0.86a	0.12a	0.14a	0.15a
H	2.44a	2.52b	2.37b	0.17a	0.16a	0.15b	0.75a	0.54b	0.67b	0.11b	0.07a	0.07b
$LSD_{0.05}$	0.13	0.12	0.24	0.04	0.02	0.02	0.04	0.15	0.18	0.00	0.08	0.07

Means (*n=4*) followed by the same letter in the same column are not significantly different from one another at the 5% significance level according to LSD test. *M = Munchong, H = Holyrood; **C1 = RRIM 2001, C2 = RRIM 2025, C3 = RRIM 3001.

Table 3. Leaf nutrient contents after one year's growth (comparing performance of clones on each soil series).

-	N (%)		P (%)		K (%)		Mg (%)	
Clone	M*	H**	M	H	M	H	M	H
RRIM 2001	2.52b	2.44ab	0.17a	0.17a	0.78a	0.75a	0.12a	0.11a
RRIM 2025	2.80a	2.52a	0.17a	0.16a	0.83a	0.67b	0.14a	0.07ab
RRIM 3001	2.85a	2.37b	0.19a	0.15a	0.86a	0.54c	0.15a	0.06b
$LSD_{0.05}$	0.19	0.14	0.02	0.01	0.15	0.05	0.03	0.04

*M = Munchong, **H = Holyrood. Means (*n=4*) followed by the same letter in the same column are not significantly different from one another at the 5% significance level according to the LSD test.

Table 4. Leaf nutrient sufficiency (%) classification of the three clones in comparison with critical nutrient levels for immature rubber.

Clone	Nutrient	Soil series			
		Munchong	Literature classification*	Holyrood	Literature classification*
RRIM 2001	N	2.52	Deficient	2.44	Deficient
	P	0.17	Deficient	0.17	Deficient
	K	0.78	Deficient	0.75	Deficient
	Mg	0.12	Deficient	0.11	Deficient
RRIM 2025	N	2.80	Deficient	2.52	Deficient
	P	0.17	Deficient	0.16	Deficient
	K	0.83	Deficient	0.67	Deficient
	Mg	0.14	Deficient	0.07	Deficient
RRIM 3001	N	2.85	Deficient	2.37	Deficient
	P	0.19	Sufficient	0.15	Deficient
	K	0.86	Deficient	0.54	Deficient
	Mg	0.15	Deficient	0.06	Deficient

*Nutrient sufficiency levels (%):- N: 3.10-3.60; P: 0.18-0.25; K: 0.97-1.40; Mg: 0.22-0.28
Note: Literature classification [2, 13]

CEC. Low nutrient content in plant tissue indicates that insufficient amounts of nutrients were absorbed and/or supplied [7]. In this study, the nutrients supplied would be in the same amount in all the treatments, but the plants grown in Munchong series soil did not give similar response to that of plants grown in the Holyrood series soil. It is obvious that nutrients supplied were not fully available to the plants due to the different soil properties. Based on these results, it is suggested that different fertilizer practices should be used for soils of contrasting texture, such as using split fertilizer application and mulching for sandy soils.

***Hevea* nutrition**

Each of the nutrients analyzed was compared with the standard range of the nutrient in immature rubber leaves which is called the 'critical nutrient value'. These critical nutrient values normally have a range which separates the level of nutrient content into three basic levels: deficient (low), sufficient (medium), and excess (high). Table 4 shows the classification of the nutrient content according to the treatment. It appears that all the plants had insufficient nutrients, except for P in RRIM 3001 planted in Munchong series soil. Although in the deficient range, not all of these plants showed visual deficiency symptoms. Some of the plants had foliar nutrient contents which were just below the sufficient range (e.g. P contents in RRIM 2001 in both soils), and no visual symptoms were observed. However, some others showed visual symptoms of nutrient deficiencies (Figs 1 and 2).

Potassium deficiency symptoms usually occur in the lower storey or older leaves and show up as yellowing of the leaf margins. This chlorosis from the leaf margins will spread inwards until the whole leaf turns yellow [2, 6, 18]. Magnesium deficiency symptoms are observed also in the lower storey leaves. Chlorosis occurs in the interveinal areas of the leaf. As magnesium is a main component in chlorophyll, chlorosis occurs when this element is absent or very limited. The green interveinal areas will fade and turn yellow; as it progresses, the leaf takes on a 'herring-bone' appearance [2, 18].

Potassium deficiency occurs when the potassium content in the soil is low, and when applied potassium is easily leached out into groundwater [16]. It was observed that plants of the clone RRIM 3001 were more susceptible to magnesium deficiency. The deficiency symptoms were more obvious in plants in the light textured soil, as the ability of the soil to supply and retain the nutrient applied was very limited [2, 18]. Although showing low performance in terms of nutrient status, the RRIM 3001 clone has been reported to show better growth than the other two clones elsewhere [7, 8].

Figure 1: Potassium deficiency symptom observed in RRIM 2025.

Figure 2: Magnesium deficiency symptom observed in RRIM 3001.

CONCLUSION

It may be concluded that the heavier textured clayey soil of the Munchong series was much better than the lighter textured sandy soil of the Holyrood series in supplying and retaining nutrients for plant uptake. The RRIM 3001 rubber clone performed as well as other two clones in terms of nutrient uptake in clayey soil except for N uptake, but was more affected when grown in sandy soil. From the results, it may also be concluded that contrasting soil texture influences the nutrient status in rubber plants, and this effect is more marked in certain clones. In order to overcome this problem and to ensure that the plants will grow at an optimum level, it may be important to have different agronomic practices for soils of contrasting texture.

Acknowledgements – The researchers would like to thank Universiti Putra Malaysia for the technical and financial assistance under the Research University Grant Scheme (RUGS) No: 01-02-12-1677RU, and also the Ministry of Higher Education (MoHE) for the research grant under the Fundamental Research Grants Scheme (FRGS), No: 07-01-12-1121FR, for supporting the research work.

REFERENCES

1. Threadingham D., Obrect W., Wieder W., Wachholz G. and Engehausen R. (2011) Rubber. 3. Synthetic rubbers, introduction and overview. In *Ullmann's encyclopedia of industrial chemistry*. Wiley-VCH, Weinheim.
2. Noordin W.D. (2012) *Rubber Plantation: Soil Management & Nutritional Requirements*. UPM Press, Serdang.
3. Shamshuddin J. and Noordin W.D. (2011) Classification and management of highly weathered soils in Malaysia for production of plantation crops. In Burcu Özkaraova Güngör (eds.) *Principles, application and assessment in soil science* pp. 75-86. InTech, Croatia.
4. Noordin W.D. (1988) Distribution, properties and classification of soils under rubber. In Jalil A. (eds.) *RRIM training manual on soils, management of soils and nutrition of Hevea* pp. 29-49. Rubber Research Institute of Malaysia, Kuala Lumpur.
5. Noordin W.D. (1975) *Pedological Study of Some Shale Derived Soils of Peninsular Malaysia*. M.Sc. thesis, State University of Ghent, Belgium.
6. Malaysian Rubber Board (2009) *Rubber Plantation and Processing Technologies*. Malaysian Rubber Board, Kuala Lumpur.
7. Shafar J.M., Noordin W.D. and Fauziah C.I. (2012) Response of *Hevea brasiliensis* (RRIM 2001) to different rates of fertilizer planted on an Oxisol. *Malaysian Journal of Soil Science* **16:** 57-69.
8. Shafar J.M., Noordin W.D. and Nazera A. (2011) Performance of *Hevea brasiliensis* as affected by different water regimes. *American Journal of Applied Sciences* **8**(3): 206-211.
9. Sheldrick B.H. and Wang S. (1993) Particle size distribution. In Carter, M.R (eds.) *Soil sampling and methods of analysis* pp. 499-511. Lewis Publishers, Boca Raton.
10. Merry R.H. and Spouncer L.S. (1988) The measurement of carbon in soils using a microprocessor-controlled resistance furnace. *Communication in Soil Science and Plant Analysis* **19**: 707-720.
11. Bremner J.M. and Mulvaney C.S. (1988) Nitrogen-total. In Page A.L., Miller R.H., and Keeny D.R.(eds.) *Methods of soil analyses. Part 2. Chemical and Microbiological Properties-Agronomy* pp. 595-622. American Society of Agronomy, Madison, WI.
12. Thomas G.W. (1982) Exchangeable Cations. In Page A.L., Miller R.H., and Keeny D.R.(eds.) *Methods of soil analyses. Part 2. Chemical and Microbiological Properties-Agronomy* pp. 159-165. American Society of Agronomy, Madison, WI.
13. Rubber Research Institute of Malaysia (1990) *Manual for Diagnosing Nutritional Requirements for Hevea*. Vinlin Press Sdn Bhd, Kuala Lumpur.
14. Noordin W.D. (1980) *The Use Discriminatory Recommendations of Fertilizers for Hevea need to be Reconsidered*. D.Sc. thesis (minor), State University of Ghent, Belgium.

15. Noordin W.D. and Shamshuddin J. (2011) Actual and potential soil capability index of Inceptisols and Entisols for rubber plantation. In Noordin W.D., Puteh A. and Yaapar N. (eds.) *Recent advances in crop science Vol. 1* pp. 265-277. UPM Press, Serdang.
16. Shamshuddin J. and Fauziah C.I. (2010) *Weathered Tropical Soils: The Ultisols & Oxisols*. UPM Press, Serdang.
17. Zainol E. (1988) Factor influencing soil formation. In Jalil, A. (eds.) *RRIM training manual on soils, management of soils and nutrition of Hevea* pp. 13-26. Rubber Research Institute of Malaysia, Kuala Lumpur.
18. Shorrocks V.M. (1964) *Mineral Deficiencies in Hevea and Associated Cover Plants*. Rubber Research Institute of Malaya, Kuala Lumpur.

Journal of Science and Technology in the Tropics (2013) 9: 25-30

Effect of dietary copper on feed intake, laying performance and egg yolk cholesterol content of Lohmann Brown hens

H. K. Wong*, I. J. Farahiyah and M. Mardhati
Strategic Livestock Research Centre, Malaysian Agricultural Research and Development Institute, GPO Box 12301, 50774 Kuala Lumpur, Malaysia
(*E-mail: hkwong@mardi.gov.my)

Received 16-01-2013; accepted 24-02-2013

Abstract A 12-week study to evaluate the effects of dietary copper (Cu) on egg production, feed efficiency and egg cholesterol content of Lohmann Brown hens was conducted. The layers (aged 30 weeks) were randomly allocated the following five dietary treatments: (1) control diet; (2) control diet supplemented with 40 mg Cu/kg diet; (3) control diet supplemented with 80 mg Cu/kg diet; (4) control diet supplemented with 120 mg Cu/kg diet; and (5) control diet supplemented with 160 mg Cu/kg diet. Daily feed consumption per bird was significantly lower (LSD, $p<0.05$) in Treatment 5 compared with Treatments 1, 2 and 3. Egg production was significantly higher (LSD, $p<0.05$) in Treatment 5 compared with the other treatments. Feed conversion ratio was significantly lower (LSD, $p<0.05$) in Treatment 5 compared with Treatments 1, 2 and 3 reflecting better feed efficiency with higher Cu supplementation. Although egg cholesterol content was lowest in Treatment 5, the differences were not significantly different (LSD, $p>0.05$) between treatments. This study shows that dietary Cu supplementation at 160 ppm can improve egg production and feed efficiency but does not reduce egg cholesterol content.

Keywords dietary copper – egg yolk cholesterol – feed efficiency – egg production

INTRODUCTION

In terms of growth promotion and improvement of animal performance, high levels of copper (175mg/kg) have been reported to promote growth of piglets. The European Commission [1] allows a level of 175 mg copper/kg in diets for piglets. Evidence that copper produces a growth-promoting effect through the microbial gut flora is supported by the results of Shurson *et al*. [2], who observed a positive effect from a high concentration of copper in the diet on the daily growth rate and feed conversion rate in conventional pigs, and a negative effect in germ-free pigs. Several observations [1, 3] show that levels of copper sulphate incorporated in diets reduced Gram positive bacterial populations in the gut.

Several dietary approaches for reducing egg cholesterol have been extensively reviewed by Elkin [4], and the same author [5] has highlighted in an editorial in the Poultry Science journal that considerable inter-laboratory variation in reported egg yolk cholesterol contents and the wide range of values cited suggest the existence of serious methodological problems in laboratories.

High dietary levels of Cu were reported to reduce egg cholesterol content although the effect was quite variable due to the laboratory assay procedures and resultant variability in baseline levels of cholesterol found in normal eggs [6]. Balevi and Coskun [7] reported a 25% reduction in yolk cholesterol in response to feeding with 150 ppm Cu. However Lim *et al.*[8] recorded only a 7% decline in response to 200 ppm dietary Cu, although this was associated with a 23% decline in serum cholesterol of these birds. Pesti and Bakalli [9] showed a slight increase in egg Cu in response to feeding with 125 ppm Cu although cholesterol content declined from 11.7 to 8.6 mg/g yolk with no further decline from feeding twice this amount of Cu. Lien *et al*. [10] needed 250 ppm rather than 125 ppm Cu to obtain a measurable change in egg composition.

Pesti and Bakalli [11] and Konjufca *et al*. [12] have reported changes in lipid metabolism and reductions in plasma and meat cholesterol concentrations of young broiler chickens due to supplementation with pharmacological levels of cupric sulphate. The changes observed in broiler chickens were consistent with observations in pigs made by Amer and Elliot [13]. Pearce *et al*. [14] demonstrated that pharmacological levels of Cu (250 mg/kg diet) caused changes in 17b-estradiol and enzymes involved in carbohydrate, lipid and amino acid metabolism in mature laying hens. Their data suggest that Cu supplements can affect reproductive physiology and lipid metabolism beyond changes simply due to reduced feed intake. Copper supplements decreased plasma lipids, 17b-estradiol and liver lipid concentrations as well as hepatic lipogenic enzyme activities. Copper is usually fed commercially at high pharmacological levels (100 to 300 mg/kg) to swine because of its growth-promoting properties [11].

The objective of this study was to determine whether pharmacological levels of Cu in laying hen diets affected feed intake, egg production, feed efficiency and egg cholesterol content.

MATERIALS AND METHODS

A total of 125 Lohmann Brown layers (aged 30 weeks, 5 pullets/replicate and 5 replicates/treatment) raised under open housing and kept in individual cages (size 450 mm X 260 mm) were used for the feeding trial.

The following five dietary treatments were fed to the hens over a 12-week period: Treatment 1 (Control), a typical corn-soybean meal based diet (Table 1);

Treatment 2, control diet with 40 ppm Cu from copper(II) sulphate pentahydrate ($CuSO4.5H_2O$); Treatment 3, control diet with 80 ppm Cu from CuSO4.5H2O; Treatment 4, control diet with 120 ppm Cu from $CuSO4.5H_2O$; Treatment 5, control diet with 160 ppm Cu from $CuSO4.5H_2O$. Calculated nutrients in the control diet are shown in Table 1.

The birds were randomly assigned and given the feed and water *ad libitum.* Feed intake data for each replicate were collected weekly over the 12 weeks (Week 31-42) and pooled to give mean feed intake for each replicate over the period. Eggs were collected and counted daily. All eggs produced on days 7, 14, 21, 28, 35, 42, 49, 56, 63, 70, 77 and 84 were weighed and pooled to give mean egg weight for each replicate over the period.

On the 12th week, egg samples were analyzed for total cholesterol using the direct saponification method of Fletouris *et al*. [15]. A Perkin Elmer Clarus 500 gas chromatograph equipped with auto-sampler and autoinjector was used to measure egg cholesterol with 5a-cholestane as the internal standard. Data were analyzed by analysis of variance using the ANOVA procedure of SAS [16] and the means compared using the LSD test.

Table 1. Layer feed formulation and nutrient composition (as-fed basis)**.**

Ingredient	% in diet	Nutrient composition in diet	
Corn	45.42	Crude protein (%)	16.80
Soybean meal	21.45	Metabolizable energy (MJ/kg)	11.18
Limestone	10.20	Crude fat (%)	4.40
Wheat middlings	10.00	Calcium (%)	4.00
Rice bran	8.00	Available phosphorus (%)	0.38
Corn gluten meal	1.76	Lysine (%)	0.93
Dical. phosphate	1.29	Methionine (%)	0.46
Palm oil	1.00	Methionine + Cystine (%)	0.74
Common salt	0.35	Threonine (%)	0.63
L-Lysine HCl	0.14	Tryptophan (%)	0.20
DL-Methionine	0.20	Linoleic acid (%)	1.50
Mineral premix*	0.10	Choline (mg/kg)	1400
Choline Cl – 70%	0.06	Sodium (%)	0.16
Vitamin premix**	0.03	Chloride (%)	0.25

*Gladron mineral premix providing per kg of ration at 1 kg/ton inclusion: 80 g iron, 100 g manganese, 15 g copper, 80 g zinc, 1 g iodine, 0.2 g selenium, 0.25 g cobalt, 4 g potassium, 0.6 g magnesium and 1.5 g sodium

** Lutamix vitamin premix providing per kg of ration at 300g/ton inclusion: 50 million IU vit. A, 10 million IU vit. D3, 75 g vit. E, 20 g Vit. K3, 10 g vit. B1, 30 g vit. B2, 20 g vit. B6, 0.1 g vit. B12, 60 g calcium D-pantothenate, 200 g niacin, 5 g folic acid and 235 mg biotin.

RESULTS AND DISCUSSION

Daily feed intake per bird (Table 2) was significantly lower in Treatment 5 ($p<0.05$) compared with the control and Treatments 2 and 3, but not significantly different ($p>0.05$) from Treatment 4. Egg production (Table 2) was significantly higher ($p<0.05$) in Treatment 5 compared with the other treatments.

The increase in egg production observed from feeding Cu supplements at 160 ppm was also reported by Jackson [17], where the highest level of egg production was observed from feeding 256 mg Cu/kg. Increasing Cu supplementation can also have detrimental effects as other authors [14, 18] have concluded that feeding with very high levels of Cu (>500 mg Cu/kg) depresses egg production.

There were no significant differences ($p>0.05$) in mean egg weight between the treatments suggesting that Cu supplementation does not affect egg size.

Data on total feed intake (Table 2) mirrored the data on daily feed intake, with feed intake significantly lower in Treatment 5 ($p<0.05$) compared with the control, Treatments 2 and 3, but was not significantly different ($p>0.05$) from Treatment 4. Total egg weight (Table 2) production per bird was significantly higher ($p<0.05$) in Treatment 5 compared with the other treatments, reflecting better feed efficiency at higher Cu supplementation. Better feed efficiency resulted in better feed conversion ratio (Table 2) showing significantly lower ($p<0.05$) readings in Treatment 5 compared with the control and Treatments 2 and 3, but was not significantly different ($p>0.05$) from Treatment 4; thus, feed conversion ratio was better with higher Cu supplementation.

Supplementation with Cu had no effect on yolk weight and cholesterol concentration in the yolk (Table 3). Egg cholesterol content was lowest in Treatment 5 but the differences were not significantly different ($p>0.05$) between the treatments (Table 3).

Table 2. Effect of copper supplementation on daily and total feed intake, egg production, egg weight and feed conversion ratio.

Treatment	1	2	3	4	5
Daily feed intake per bird (g/day)	107.32^{a}	107.20^{a}	107.47^{a}	107.00^{a}	106.74^{b}
Total feed intake per bird (kg per 12 weeks)	9.02^{a}	9.00^{a}	9.03^{a}	8.99^{ab}	8.96^{b}
Egg production (%)	91.35^{a}	91.16^{a}	91.10^{a}	91.90^{a}	92.73^{b}
Egg weight (g)	61.36^{a}	61.54^{a}	61.82^{a}	61.56^{a}	61.58^{a}
Total egg weight per bird (kg per 12 weeks)	4.71^{a}	4.71^{a}	4.73^{a}	4.75^{a}	4.80^{b}
Feed conversion ratio	1.91^{a}	1.91^{a}	1.91^{a}	1.89^{ab}	1.87^{b}

Values within a row and bearing different letters are significantly different from one another according to the LSD test ($p< 0.05$)

Table 3. Effect of copper supplementation on yolk weight, yolk cholesterol concentration and total yolk cholesterol.

Treatment	1	2	3	4	5
Yolk weight (g)	14.84[a]	14.73[a]	14.90[a]	14.66[a]	14.37[a]
Yolk cholesterol concentration (mg/g yolk)	12.00[a]	11.77[a]	11.80[a]	11.68[a]	11.56[a]
Total yolk cholesterol (mg/yolk)	177.96[a]	173.35[a]	175.70[a]	171.24[a]	166.13[a]

Values within a row and bearing different letters are significantly different from one another according to the LSD test ($p< 0.05$)

de Mendonca[19] fed laying hens a commercial diet supplemented with copper sulphate at levels of 200, 400, 600 and 800 mg of Cu/kg for a period of 6 weeks, and reported that egg weight, egg production, feed intake and feed conversion were not significantly affected by the supplemental copper up to 400 ppm. At 600 and 800 mg/kg copper significantly reduced egg weight, egg production and feed intake. Contrary to the reports by Pesti and Bakalli [11] on feeding with 125 and 250 ppm Cu and Balevi and Coskun [7] on feeding with 150 ppm Cu, de Mendonca [19] reported that feeding supplemental copper had no effect on egg yolk cholesterol, and that supplemental copper at 800 ppm significantly increased egg yolk cholesterol.

In this study, supplementation for up to 12 weeks with 160 ppm Cu had improved egg production and feed efficiency but had no significant effect on egg cholesterol content.

REFERENCES

1. European Commission, Health & Consumer Protection Directorate-General (2003) *Opinion of the Scientific Committee for Animal Nutrition on the use of copper in feeding stuffs*.
2. Shurson G.C., Ku P.K., Waxler G.L., Yokoyama M.T. and Miller E.R. (1990) Physiological relationships between microbiological status and dietary copper in the pig. *Journal of Animal Science* **68**: 1061-1071.
3. Dunning J.C. and Marquis R.E. (1998) Anaerobic killing of oral streptococci by reduced, transition metal cations. *Applied Environmental Microbiology* **64**: 27-33.
4. Elkin R.G. (2007) Reducing shell egg cholesterol content. II. Review of approaches utilizing non-nutritive dietary factors or pharmacological agents and an examination of emerging strategies. *World's Poultry Science Journal* **63** (1): 5-32.
5. Elkin R.G. (2009) Additional perspectives on analytical techniques and standardization: Cholesterol and fatty acid contents of eggs, tissues, and organs. *Poultry Science* **88**: 249-2503.
6. Leeson S. (2009) Copper metabolism and dietary needs. *World's Poultry Science Journal* **65**: 353-366.
7. Balevi T. and Coskun B. (2004) Effects of dietary copper on production and egg cholesterol content in laying hens. *British Poultry Science* **45:** 530-534.

8. Lim K.S., You S.J., An B.K. and Kang C.W. (2006) Effects of dietary garlic powder and copper on cholesterol content and quality characteristics of chicken eggs. *Asian-Australian Animal Science* **19**: 582-586.
9. Pesti G.M. and Bakalli R.I. (1998) Studies on the effect of feeding cupric sulfate pentahydrate to laying hens on egg cholesterol content. *Poultry Science* **77**:1 540-1545.
10. Lien T.F., Chen K.L., Wu C.P. and Lu J.J. (2004) Effects of supplemental copper and chromium on the serum and egg traits of laying hens. *British Poultry Science* **45**: 535-539.
11. Pesti G.M. and Bakalli R.I. (1996) Studies on the feeding of cupric sulfate pentahydrate and cupric citrate to broiler chickens. *Poultry Science* **75**: 1086-1091.
12. Konjufca V.H., Pesti G.M. and Bakalli R.I. (1997) Modulation of cholesterol levels in broiler meat by dietary garlic and copper. *Poultry Science* **76**: 1264-1274.
13. Amer M.A. and Elliot J.I. (1973) Effects of supplemental dietary copper on glyceride distribution in the backfat of pigs. *Canadian Journal of Animal Science* **53**: 147-152.
14. Pearce J., Jackson N. and Stevenson M.H. (1983) The effects of dietary intake and of dietary concentration of copper sulphate on the laying domestic fowl: Effects of some aspects of lipid, carbohydrate and amino acid metabolism. *British Poultry Science* **24**: 337-348.
15. Fletouris D.J., Botsoglou N.A., Psomas E. and Mantis A.I. (1998) Rapid determination of cholesterol in milk and milk products by direct saponification and capillary gas chromatography. *Journal of Dairy Science* **81**: 2833-2840.
16. SAS Institute Inc. (2000) SAS/STAT *User's Guide*. SAS Institute Inc., Cary, NC.
17. Jackson N. (1977) The effect of dietary copper sulphate on laying performance, nutrient intake and tissue copper and iron levels of the mature, laying, domestic fowl. *British Journal of Nutrition* **38**: 93-100.
18. Stevenson M.H., Pearce J. and Jackson N. (1983) The effects of dietary intake and of dietary concentration of copper sulphate on the laying domestic fowl: Effects on laying performance and tissue mineral contents. *British Poultry Science* **24**: 327-335.
19. de Mendonca C.X, Jr. (1999) Effects of high supplemental dietary copper on laying performance, egg yolk cholesterol and blood plasma lipids. *Brazilian Journal of Veterinary Research and Animal Science* **36** (6): (online at http://www.scielo.br/scielo.php?)

Journal of Science and Technology in the Tropics (2013) 9: 31-45

Comparison of *Acropora formosa* coral growth in natural habitat condition between Tioman Island and Pangkor Island, Malaysia

Loke Hai Xin,[1,*] Alvin Cheliah,[2] Chen Sue Yee,[2] Julian Hyde,[2] Zaidi Che Cob,[1] and Kee Alfian Abdul Adzis[1]

[1]Faculty of Science and Technology, National University of Malaysia, 43600 UKM, Bangi Selangor, Malaysia
(*Email: lokehx@gmail.com)
[2]Reef Check Malaysia, Suite 5.19-5.22, Box 606, Wisma Central, Jalan Ampang, 50450 Kuala Lumpur, Malaysia

Received 08-04-2013; accepted 19-04-2013

Abstract *Acropora formosa*, a reef-building coral abundant in Tioman Island and Pangkor Island was studied for its extension growth (extension of the main branch) and proto-branch generation (frequency of new axial branch generated from the main branch) in its natural reef habitat. Measurements of extension growth using flexible measuring tape and observations of proto-branch generation were conducted every two months for a period of six months. The chosen sites were Pulau Renggis in Tioman Island and Pangkor Laut in Pangkor Island. Additional measurements of photosynthetic yield (ΔF/Fm') using diving PAM and parameters (PAR light intensity, Secchi disk visibility and temperature) were recorded respectively. The extension growth of *A. formosa* was better in Pangkor Laut (3.91 ± 2.37cm) than Pulau Renggis (2.32 ± 1.62cm) after six months. The proto-branch generation rate was also higher in Pangkor laut (59.09%) than in Pulau Renggis (19.23%). The factors affecting this outcome and growth comparisons between other studies were discussed.

Keywords *Acropora formosa* – coral growth – Tioman Island – Pangkor Island

INTRODUCTION

The rapid and worldwide decline of coral reefs in recent decades caused by various factors such as climate change, coral bleaching, pollution, sedimentation, overfishing and coral mining, has raised concerns across the nations. Studies have been conducted to look into the health of the coral reefs around the globe to comprehend their conditions [1-3].

Malaysia is a country within the Coral Triangle and holds abundant coral species, as rich as 323 species [4]. Both the west and east coast of Peninsular Malaysia have islands rich in marine life. Many of these islands are highly economical for developing tourism, e.g. Pangkor Island within the Malacca

Straits and Tioman Island within the South China Sea [5]. The reef coverage in these two islands ranges from 17.9% to 68.6% [6]. The pressure of island tourism and development over time, such as coral reef damage by overcrowding tourists and snorkelers, beach degradation, sewage and solid waste disposal, has brought negative effects upon the reefs in many of these islands [5, 7].

Tioman Island is famous as one of the most attractive snorkel and dive sites in the world and was one of the locations for the musical film 'South Pacific'. Tourism development started since early 1970s and resort hotels flourish then. It is located about 32 nautical miles east from Tanjung Gemuk, Pahang. The island group and its surrounding waters were gazetted as a Marine Park in 1994 under the Fisheries Act 985 (Amended 1993). It is also one of the islands that can be easily accessed through flight from Kuala Lumpur and Singapore. Tioman Island is affected by the seasonal Northeast Monsoon from November to February [5, 8].

Pangkor Island is noted for its fishing industry which is centered on the island's east coast. It is also a famous weekend and holiday getaway. Accommodation units first appeared in late 1960s from small-scale units, until increasing amount of resort hotels by late 1980s, not only on Pangkor Island but also on the smaller neighbouring Pangkor Laut Island [5].

Corals of the genus *Acropora* are dominantly found in both Tioman Island and Pangkor Island [6]. A previous 2010 study [9] had identified the species to be *Acropora formosa*, which was also the same targeted species at the sites for this study. This species is notably known as one of the fast growing staghorn corals on reefs, and excellent reef-builders [10]. The colonies could form extensive and complex thickets as dense as 1.5 m high with even and fairly regular branch surfaces [11], thus suitable and convenient for the tagging and measuring work of this study.

It is generally observed that, the water surrounding Pangkor Island is very green and murky, while the water in Tioman Island especially the dive sites is clear and suitable for leisure diving. Previous studies [12, 13] stated there was close relation between light intensity and scleractinian coral calcification and growth. Thus this study aimed to investigate the coral growth in the two sites of different environment condition.

In order to monitor these reefs' health, previous studies and surveys through approach of coral distribution, community structure and photosynthetic yield had been done [3, 4, 6, 9, 14]. However a review in 2012 [7] pointed out that, studies in terms of qualitative, quantitative and bio-geographical data of the reefs in Malaysian waters were scarce. Coral growth rates, commonly in the aspect of extension rate [15-18], are often used in environment assessment as direct indicator of the reef health [19, 20]. Coral growth rate was suggested as a standard ecological tool to determine growth tolerances of reef-building

organisms [21]. Hence this study took the approach of coral growth to investigate *A. formosa* condition in these two islands.

Other than monitoring the extension growth rate of *A. formosa*, this study also recorded the observation of new axial branch or proto-branch [22] formation and survival rate to be analyzed, as both of these factors were part of coral growth study [16, 18, 23, 24]. The effective quantum yields of the zooxanthellar photosynthesis were measured, which photosynthetic rate was closely related with energy production and growth, as health indicator for the tagged coral branches [14, 25, 26]. Since the synergistic effects of environment parameters were important factors for corals [27], water temperature and light intensity were recorded for baseline information of the sites' environment. With the combined information, this study aimed to obtain an elaborating and comparable growth rate profile of *A. formosa* in Tioman Island and Pangkor Island.

MATERIALS AND METHODS

The growth rate of *A. formosa* was studied from the aspect of the coral branch's extension. Additional observation of proto-branch generation and mortality was recorded. A minimum six months monitoring period was conducted with measuring intervals of two months. The sample size of coral branches in Tioman Island was N=30, monitoring since 4th June 2012; that of Pangkor Island was N=60, started since 15th March 2012. Task of monitoring was carried out *in situ* using SCUBA.

Site description

One coral reef site was chosen at Tioman Island and Pangkor Island for this study. In Tioman Island, the site was at Pulau Renggis (N 2° 48' 36.16", E 104° 8' 10.13"), with live coral cover as high as 68.6% [6]. The average depth of the site was 6.48 ± 0.55 m. The salinity range was documented between 30.02 ppt and 30.57 ppt [28], but during this study period, salinity was recorded up to 34 ppt.

In Pangkor Island, the site was at Pangkor Laut Island (N 4° 11' 25.73", E 100° 32' 50.58"), with up to 50% of hard coral cover [29]. The average depth of the site was 3.66 ± 0.94 m. The salinity ranged from 29 to 32 ppt [30].

Tagging

Both study sites were marked with underwater buoys. Healthy *A. formosa* branches near the buoys were selected and marked with plastic cable ties. Each branch was tied at a range of >2 cm from the branch tip. Each cable tie was attached together with a fragment of numbered plastic tape as tag. During each visit, the silts and foulers on the plastic tag surfaces were cleared.

Extension growth

The growth extension of coral branch was monitored using direct measurement. A fragment of flexible measuring tape was used to align with the tagged branch. Then linear measurement was taken starting from the plastic tag until the tip of the main branch's axial end. The measurement reading was recorded to the nearest tenth of centimeters. Across the six months period, the cumulative growth extensions for every two months were measured and the extension rates during each of the three intervals between visits were calculated.

Proto-branch and survival observation

After a period of growth, the tagged branches might generate proto-branches. Extension length for these proto-branches was not measured; however the frequencies of the proto-branches generated by tagged main branches were counted and recorded. Any mortality or fragment broken off of the branches were observed and recorded. In case of complete mortality of the tagged branch, the mortality frequency was noted for survival rate calculating.

Chlorophyll fluorescence and environmental factors

At ambient temperatures, chlorophyll fluorescence in algae and plants emanates almost exclusively from antennae pigments of photosystem II. The initial or constant fluorescence, F_0, of the samples signifies fluorescence when the reaction centres of photosystem II are fully oxidized. When a saturating pulse of white light is applied causing reduction of the photosystem II reaction centres, fluorescence increases to a maximal value Fm. In light adapted condition, which was also the condition of this study when carrying out the measurement, the values of F_0 and Fm changed, resulting in F and Fm'. Providing the equation, $(Fm'-F)/Fm' = \Delta F/Fm'$, where Fm' is maximum fluorescence yield in the given light state, and F the steady state fluorescence yield in this particular state monitored briefly before the saturation pulse, and the change in fluorescence ΔF could be measured *in situ* by using an underwater pulse amplitude modulated (PAM) fluorometer (the Diving-PAM, Walz Gmbh, Germany). The value of $\Delta F/Fm'$ is known as effective quantum yield [14, 25, 26, 31]. The operational steps of the Diving-PAM were carried out according to the instrument's handbook of operation [32].

In this study during the initial period when the branches were newly tagged at both sites, measurement of the effective quantum yield was conducted for the first time. Six months later the measurement was conducted again for the second time. This was to provide a brief understanding on the health condition of *A. formosa* branches.

Values of light intensities received by the corals during initial period and end of six months period were obtained using the internal Light-Calibration program

of the Diving-PAM [32], measuring as photosynthetic active radiation or PAR (μmol m^{-2} s^{-1}). Then the ranges of PAR reading were obtained. Visibilities of the waters were obtained by observation through Secchi disk for water turbidity readings [33].

In order to obtain continuous temperature monitoring, Onset HOBO Pendant Temperature Data Loggers were placed at both sites, by tying the logger with plastic cable tie to sessile hard bottom substrate near the buoys during the initial period of the study. Operational steps were done according to the instrument's instruction handbook [34].

Statistical analysis

Measurements of the coral extension growth were taken in centimeters, and then the cumulative growth and interval extension growth rate were calculated to be presented in means and standard deviations. The observation record of survival rate and proto-branch rate were calculated into percentage. The homogeneity of variances was confirmed by using *F* test and Bartlett's test. Then, two sample Mann-Whitney test and One-way ANOVA test were used to analyze intervals extension growth rate. Survival rate and proto-branch generation rate were tested using Paired *t*- test.

The analytical tests of this study were done by using the program Minitab version 14.1.

RESULTS

Table 1 shows the compilation results of extension growth, sample size, survival rate and proto-branches generation rate for both sites. The reduction in sample size for both sites was mainly due to increasing difficulty to relocate the same tagged branches, as these *A. formosa* branches gradually overgrew the cable ties and tags. Branches which demonstrated negative extension, due to predation by reef organisms or broken by wave action, were excluded from the sample pool in order to obtain statistical accuracy.

Extension growth

Over the six months period of this study, extension growth of *A. formosa* varied considerably with large standard deviations at both sites. In Pulau Renggis the mean cumulative extension growth was 2.32 ± 1.62 cm, and 3.91 ± 2.37 cm in Pangkor Laut (Fig. 1). The growth rates in Pangkor Laut were higher than Pulau Renggis throughout the six months especially during the second and third intervals, where Pangkor Laut's rates were nearly double of Pulau Renggis and the Two sample Mann-Whitney test (Table 2) showed significant difference ($P < 0.05$). This led to higher cumulative extension growth

Table 1. Growth extension, sample size, survival rate and proto-branch generation rate for *Acropora formosa* from Pulau Renggis and Pangkor Laut. Standard deviations are in parentheses.

Sites	Period	Sample size, N	Mean cumulative growth extension (cm)	Mean intervals extension rate (cm/month)	Survival rate (%)	Proto-branched rate (%)	Mean new proto-branches generation	Mean cumulative proto-branches generation
Pulau Renggis	Initial	30	0 (0)		100.00	0.00	0 (0)	0 (0)
				0.41 (0.36)				
	2 months	26	0.83 (0.72)		100.00	0.00	0 (0)	0 (0)
				0.32 (0.27)				
	4 months	26	1.46 (1.02)		100.00	11.54	1.67 (1.15)	1.67 (1.15)
				0.43 (0.39)				
	6 months	26	2.32 (1.62)		100.00	19.23	1.50 (0.71)	1.60 (0.89)
				Mean				
	Overall monthly growth rate (cm/month)			0.39 (0.27)				
	Assumed annual growth rate (cm/year)			4.63 (3.23)				
Pangkor Laut	Initial	60	0 (0)		100.00	8.33	0 (0)	1.20 (0.45)
				0.53 (0.43)				
	2 months	46	1.05 (0.85)		100.00	34.78	1.71 (0.99)	1.88 (0.96)
				0.87 (0.49)				
	4 months	41	2.63 (1.64)		100.00	58.54	2.44 (1.75)	2.38 (1.58)
				0.72 (0.52)				
	6 months	41	3.91 (2.37)		98.08	59.09	3.46 (2.11)	3.54 (2.70)
				Mean				
	Overall monthly growth rate (cm/month)			0.65 (0.40)				
	Assumed annual growth rate (cm/year)			7.83 (4.75)				

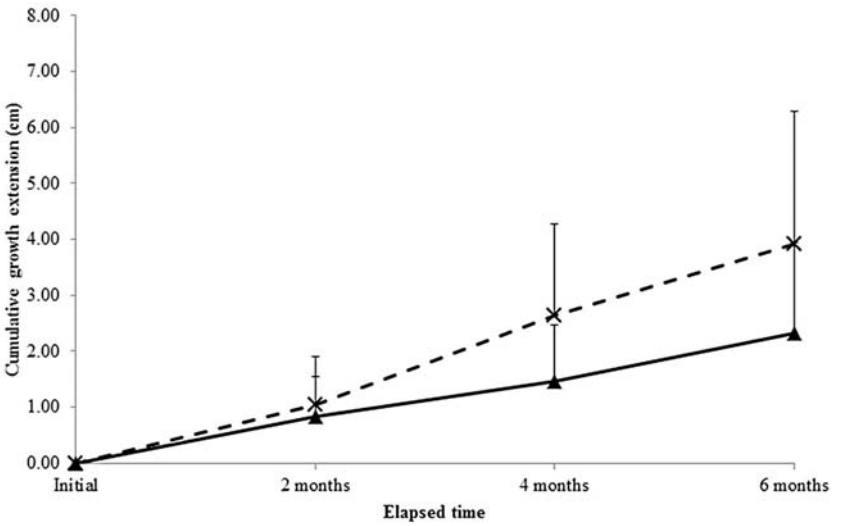

Figure 1. Cumulative growth extension of *Acropora formosa* in both sites. –▲– Pulau Renggis; –X– Pangkor Laut. Error bar represents standard deviation.

Table 2. Statistic results of comparing growth rates between Pulau Renggis and Pangkor Laut sites by intervals. Significant difference ($P < 0.05$).

	Test for equal variances, *F* test		Two sample Mann-Whitney test	
	F	*P*	*W*	*P*
First	1.41	0.358	858.0	0.2887
Second	3.34	0.002*	532.0	0.0000*
Third	1.74	0.145	702.5	0.0104*

Table 3. Statistic results of comparing growth rates between three intervals by sites. Significant difference (P<0.05) in One-way ANOVA of Pangkor Laut between first and second intervals was indicated by Tukey's Multiple Comparisons.

	Test for equal variances, Bartlett's test		One-way ANOVA			
	Statistic	DF	SS	MS	F	P
Pulau Renggis	3.70	2	0.189	0.094	0.80	0.452
Pangkor Laut	1.63	2	2.591	1.296	5.72	0.004*

* Significant difference (P<0.05).

Table 4. Frequency of Acropora formosa cumulative proto-branch generation over six months period in Pulau Renggis and Pangkor Laut.

Proto-branch amount at one tagged sample	Pulau Renggis				Pangkor Laut			
	Initial	2 months	4 months	6 months	Initial	2 months	4 months	6 months
0	30	26	23	21	55	30	17	14
1	-	-	2	3	4	7	9	7
2	-	-	-	1	1	5	6	7
3	-	-	1	1	-	3	5	2
4	-	-	-	-	-	1	1	3
5	-	-	-	-	-	-	2	4
6	-	-	-	-	-	-	-	1
7	-	-	-	-	-	-	1	-
8	-	-	-	-	-	-	-	2
9	-	-	-	-	-	-	-	-
10	-	-	-	-	-	-	-	-
11	-	-	-	-	-	-	-	-
12	-	-	-	-	-	-	-	1

in Pangkor Laut (3.91 ± 2.37 cm) than Pulau Renggis (2.32 ± 1.62 cm). However, One-way ANOVA (Table 3) analyzed intervals extension growth rate within same site showed no significant difference of changes ($P > 0.05$) for Pulau Renggis but significant difference ($P < 0.05$) for Pangkor Laut, thus suggesting *A. formosa* in Pulau Renggis was growing at a more steady rate.

Proto-branch and survival observation

Generation of proto-branches in Pangkor Laut site was surprisingly high, as more than half of the samples generated proto-branches. In Pulau Renggis, by the end of six months period approximately one-fifth of the tagged corals had generated proto-branches. The amount of proto-branches generated on one tagged branch varied largely in Pangkor Laut, ranging from 1 to 12 proto-branches after six months (Table 4). Proto-branches in Pulau Renggis were first sighted after four months since initially tagged with cable ties, and the proto-branch amount per sample ranged between one to three (Table 4). The survival rate was high in both sites; 100% for Pulau Renggis throughout the 6 months period, and only one branch died on the sixth month in Pangkor Laut. Values of

survival rate between sites were too identical to be tested for equal variance. The cumulative proto-branching rate in Pangkor Laut was significantly higher than Pulau Renggis, but no significant difference in terms of survival rate (Table 5).

Chlorophyll fluorescence and environmental factors

In Pulau Renggis, the mean value of effective quantum yield (ΔF/Fm') was 0.64 ± 0.096 at the beginning and 0.67 ± 0.111 six months later. In Pangkor Laut, the range of the mean yield value was between 0.69 ± 0.135 to 0.72 ± 0.094 (Table 6). The PAR range in Pangkor Laut was higher than Pulau Renggis, due mainly to the difference between their mean depths. Nevertheless, the visibility readings of Secchi disk at both sites showed that the Pangkor Laut water was more turbid (Table 7). The daily mean, maximum and minimum water temperatures of Pulau Renggis and Pangkor Laut were shown in Figures 2 and 3 respectively. Although the range between daily maximum and minimum water temperatures were mostly smaller for Pulau Renggis site throughout the six months period, the daily mean water temperature of Pangkor Laut site never went below 29°C.

Table 5. Statistic results of comparing cumulative proto-branch generation rate and survival rate between sites. Values of survival rate between sites were too identical to be tested for equal variance.

	Test for equal variances, *F* test		Paired *T* test	
	F	*P*	*T*	*P*
Proto-branch	7.19	0.139	3.81	0.032*
Survival	-	-	1.00	0.391

* Significant difference (P<0.05).

Table 6. Comparison of Effective Quantum Yield, ΔF /Fm' between studies. Standard deviations are in parentheses.

Study	Coral species	Location	Set	Mean yield, ΔF /Fm'	
Ralph 1999 [42]	*Acropora aspera* *Goniastrea sp.* *Porites sp.*	Heron Island, Great Barrier Reef, Australia		0.47 0.54 0.59	(0.051) (0.004) (0.019)
Negri, 2005 [54]	Acropora milipora Pocillopora damicornis	Lizard Island, Great Barrier Reef, Australia		0.52 0.43	(0.02) (0.01)
Adzis, 2009 [14]	*Pocillopora damicornis*	Tanjung Mesoh, Pulau Tioman, Malaysia	Colony 1 Colony 2	0.70 0.72	(0.05) (0.03)
Bielmyer, 2010 [55]	Acropora cervicornis Pocillopora damicornis	University of Miami, US		0.42 0.49	(0.03) (0.01)
This study, 2012	*Acropora formosa*	Pulau Renggis, Tioman Island, Malaysia	1st [a] 2nd [b]	0.64 0.67	(0.096) (0.111)
		Pangkor Laut, Pangkor Island, Malaysia	1st [c] 2nd [d]	0.72 0.69	(0.094) (0.135)

[a] $n = 101$; [b] $n = 60$; [c] $n = 120$; [d] $n = 78$

Table 7. Light intensity and visibility at Pulau Renggis and Pangkor Laut.

Site	PAR range, μmol m-2 s-1	Visibility range underwater, m	Visibility range of Secchi disk, m
Pulau Renggis [a]	30 - 175	4 – 8	> 4.6
Pangkor Laut [b]	21 - 205	1 - 5	1.70 – 1.75

[a] mean depth = 6.48 ±0.55 m; [b] mean depth = 3.66 ±0.94m.

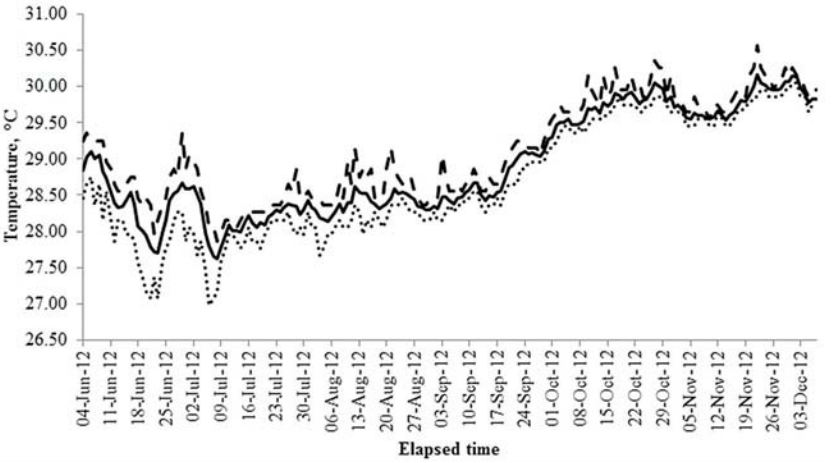

Figure 2. Three daily water temperature parameters at Pulau Renggis site during the six months study period. ——— mean; — — — maximum; ····· minimum.

DISCUSSION

The main finding of this study was the difference of extension growth, which was significantly better in Pangkor Laut compared to Pulau Renggis. There are several possible explanations. Firstly, the Pangkor Laut site, being slightly shallower and receiving relatively higher irradiance, would have allowed higher photosynthesis productivity for coral calcification and growth [12, 13]. Secondly, the patterns of daily mean water temperature in both sites were different at 29°C (Figs. 2, 3). Pangkor Laut site with better *A. formosa* growth had daily mean water temperature above 29°C throughout the six months period. In Pulau Renggis site, the daily mean water temperature was below 29°C most of the time until early October. After the daily mean water temperature exceeded 29°C during the third intervals, the extension rate improved (Table 1). Although a study in 1997 [35] mentioned that optimal water temperature range for coral reefs was 26-28°C, this study indicated that the optimal temperature range for *A. formosa* could be higher and further study is needed. With global warming, there might be a shift in the community structure of reef building coral. For

example, the abundance of *A. formosa* may increase due to higher optimal water temperature for their faster growth, and overgrow other hard corals with slower growth.

Thirdly, the water in Pangkor Laut appeared to be more turbid and greenish. Although general studies [36, 37] indicate that turbidity reduces coral growth directly, there are also studies [38, 39] showing no clear trend between turbidity and coral growth. The turbid and greenish water might be due to more organic particles and phytoplankton indicating possible higher suspension feeding for *Acropora* corals [40, 41].

Compared to other fluorescence yield studies, the photosynthetic productivity of *A. formosa* was relatively lower than *Pocillopora damicornis* in the same island (Tioman Island) [14], but was relatively better than the photosynthetic productivity of three other coral species in Australia [42]. Furthermore, the massive scale of the 1997–1998 El Niño–associated coral bleaching event would probably had obstructed the condition of corals before Ralph's study [42, 43]. Hence, the corals in this study were assumed to be in a relatively healthy state (Table 6).

The growth rates of *A. formosa* in this study (Table 8) were within the range from 0.39 ± 0.13 to 0.69 ± 0.20 cm/month in Japan [16]. Compared to Andaman Sea [15], the growth rate in Pulau Renggis was lower but Pangkor Laut was higher. In Australia [23], the growth rates were within the range between Pulau Renggis and Pangkor Laut. The growth rates of other species of *Acropora* [44-46] were mostly higher than Pulau Renggis but lower than Pangkor Laut, except *A. valenciennesi* in Kaledupa, Indonesia which was the highest (1.00 ±0.17 cm/month).

There are ongoing reef restoration projects in several islands of Peninsular Malaysia, including Tioman Island and Pangkor Island. Hence, it is necessary to investigate ecological parameters of each local reef and relation between these parameters [47] to better understand the variation of water and reef conditions which could probably contribute to the outcomes of the restoration efforts. The results in this study only serve narrow reference purpose for one species of hermatypic coral and limited parameters at two sites. It is without doubt that more studies covering different coral species, broader ecological parameters and more reef sites are needed. As growth rate is also one of essential criteria to identify resilience reef [48], the sites in this study could be further surveyed to be confirmed as resilience reef for the coral reef conservation and management efforts, or to determine suitable types of coral to be used for reef restoration at different places in Malaysia [43, 47].

This study not only showed that *A. formosa* in Pangkor Laut had a faster growth rate but also better proto-branch generation. The generation and fast growth of proto-branch is essential for forming a branching coral reef. The

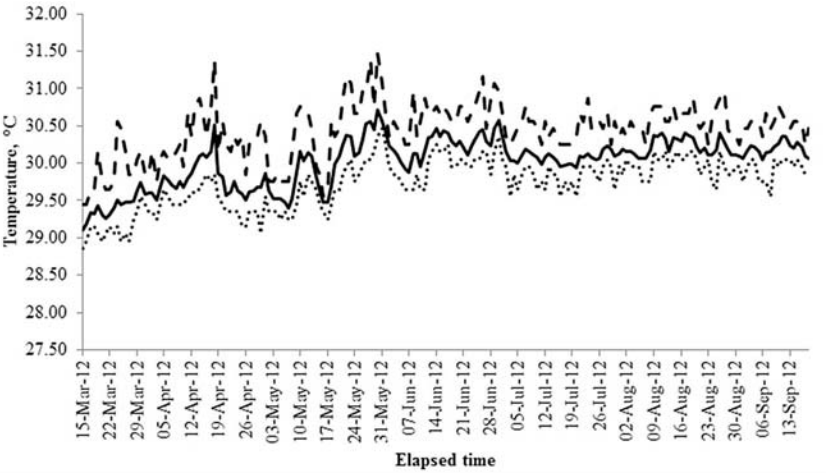

Figure 3. Three daily water temperature parameters at Pangkor Laut site during the six months study period. ——— mean; — — — maximum; ····· minimum.

Table 8. Comparison of *Acropora sp*. extension rate, cm/month between studies. Standard deviations are in parentheses.

Studies	Acropora species	Method	Site location	Set	Mean extension rate (cm/month)
Gladfelter, 1978 [45]	*A. cervicornis*	Alizarin stain	Buck Island, Virgin Islands, US		0.59 (0.05)
	A. prolifera			1	0.68 (0.03)
				2	0.49 (0.02)
Charuchinda, 1984 [15]	*A. formosa*	Direct measure with flexible ruler	PMBC Pier, Pulau Phuket, Thailand		0.51 (0.15)
Harriott, 1998 [23]	*A. formosa*	Alizarin stain	Houtman Abrolhos, Western Australia	1	0.66 (0.13)
				2	0.57 (0.15)
				3	0.51 (0.13)
				4	0.44 (0.16)
Crabbe, 2002 [44]	*A. valenciennesi*	Image analysis with flexible tape	Kaledupa, Island of Hoga, Indonesia		1.00 (0.17)
			Sampela, Island of Hoga, Indonesia		0.55 (0.13)
Okubo, 2005 [16]	*A. formosa*	Direct measure with chain	Akajima Island, Okinawa, Japan	1	0.39 (0.13)
				2	0.63 (0.14)
				3	0.69 (0.20)
Lirman, 2010 [46]	*A. cervicornis*	Direct measure with plastic ruler	Biscayne National Park, Florida, US		0.63 (0.29)
This study, 2012	*A. formosa*	Direct measure with flexible tape	Pulau Renggis, Tioman Island, Malaysia		0.39 (0.27)
			Pangkor Laut, Pangkor Island, Malaysia		0.65 (0.40)

branching structure due to proto-branch generation would bring advantage to the reef and coastal beach by reducing impact of wave action and hydrodynamic [49]. The geometry of branching colony could protect the colony against excessive light in shallow waters by modulating light levels for the reef [50]. In addition it also benefits other reef inhabitants by providing shades. A high rate of proto-branch generation would also signify high asexual reproduction through coral fragmentation, which would be essential for colony expansion [22] and regeneration after storm destruction [51]. The fragments of proto-branches could be highly utilized for coral transplantation [18, 51]. Nevertheless, Pangkor Island is currently not gazetted as a marine protected area. Because of the depletion of reef resources and the demand from local snorkeling guide [52, 53], there is urgency and need to conserve the resilience potential reef in Pangkor Island.

In conclusion, this study provides a preliminary understanding of *A. formosa* coral growth in Malaysian waters. However, continuous long term or future monitoring of coral growth is needed, in order to keep track of coral growth history pattern to archive the record for any reef dynamics. This preliminary result on *A. formosa* indicates that this species could serve as reef health indicator and also material for coral transplantation.

Acknowledgements – This work was funded by Reef Check Malaysia and partially funded by UKM Grant: AP -2012-013 to Zaidi Che Cob and FRGS Grant: UKM-ST-06-FRGS0246-2010 to Kee Alfin Abdul Adzis. We are grateful to Shahrul for his assistance. Special thanks to Tioman Dive Centre, Abect Aqua Dive, B&J Diving and Eco-Divers for supporting this project with equipment and boat trips.

REFERENCES

1. Baker A.C., Glynn P.W. and Riegl B. (2008) Climate change and coral reef bleaching: An ecological assessment of long-term impacts, recovery trends and future outlook. *Estuarine, Coastal and Shelf Science* **80**(4): 435-471.
2. Brown B.E. (1997) Disturbances to reefs in recent times. In Birkeland C. (Ed.). *Life and death of coral reefs*. pp: 354-379. International Thomson Publishing.
3. RCM (2008) *Coral Reef Monitoring Report 2008*. Kuala Lumpur: Reef Check Malaysia.
4. Harborne A., Fenner D., Barnes A., Beger M., Harding S. and Roxburgh T. (2000) *Status Report on the Coral Reef of the East Coast of Peninsular Malaysia*. Kuala Lumpur: Coral Cay Conservation Ltd.
5. Wong P.P. (1993) Island tourism development in Peninsular Malaysia: environmental perspective. In Wong P.P. (ed.). *Tourism vs Environment: The Case for Coastal Areas*, pp. 83-97. Kluver Academic Publishers.
6. Toda T., Okashita T., Maekawa T., Kee Alfian B.A.A., Rajuddin M.K.M., Kakajima R., Chen W.X., Takahashi K.T., Othman B.H.R. and Terazaki M. (2007) Community

structures of coral reefs around Peninsular Malaysia. *Journal of Oceanography* **63**: 113-123.
7. Praveena S., Siraj S. and Aris A. (2012) Coral reefs studies and threats in Malaysia: a mini review. *Reviews in Environmental Science and Bio/Technology* **11**(1): 27-39.
8. http://www.dmpm.nre.gov.my/ptl_pahang.html?&lang=en.
9. Adzis K.A.A., Amri A.Y., Hyde J., Maidin N., Repin I.M. and Mohamed C.A.R. (2012) In situ measurement of photosynthetic capacity in scleractinian corals (*Acropora formosa* and *Pocillopora damicornis*) during the 2010 massive coral reef bleaching event in Pulau Tioman, Malaysia. *Journal of Science and Technology in the Tropics* **8**: xx-xx.
10. Veron J.E.N. (1986) *Corals of Australia and the Indo-Pacific*. Angus & Robertson Publishers, UK.
11. http://www.marinespecies.org/aphia.php?p=taxdetails&id=207036.
12. Goreau T.F. (1959) The physiology of skeleton formation in corals, I. A method for measuring the rate of calcium deposition under different conditions. *Biol. Bull.* **116**: 59-75.
13. Strömgren T. (1987) The effect of light on the growth rate of intertidal Acropora pulchra (Brook) from Phuket, Thailand, lat. 8°N. *Coral Reefs* **6**(1): 43-47.
14. Adzis K.A.A., Amri A.Y., Oliver J. and Mohamed C.A.R. (2009) Effective and maximum quantum yield of the lace coral *Pocillopora damicornis* (Anthozoa: Scleractinia: Pocilloporidae) in Pulau Tioman, Malaysia. *Journal of Science and Technology in the Tropics* **5**(1): 13-17.
15. Charuchinda M. and Hylleberg J. (1984) Skeletal extension of *Acropora formosa* at a fringing reef in the Andaman Sea. *Coral Reefs* **3**(4): 215-219.
16. Okubo N., Taniguchi H. and Motokawa T. (2005) Successful methods for transplanting fragments of *Acropora formosa* and *Acropora hyacinthus*. *Coral Reefs* **24**(2): 333-342.
17. Oliver J. (1984) Intra-colony variation in the growth of *Acropora formosa*: extension rates and skeletal structure of white (Zooxanthellae-free) and brown-tipped branches. *Coral Reefs* **3**(3): 139-147.
18. Soong K. and Chen T.-A. (2003) Coral transplantation: Regeneration and growth of *Acropora* fragments in a nursery. *Restoration Ecology* **11**(1): 62-71.
19. Eakin M.C., Feingold J.S. and Glynn P.W. (1994) Oil refinery impacts on coral reef communities. In Aruba N.A. (Ed.) *Proceedings of the Colloquium on Global Aspects of Coral Reefs: Health Hazards and History*, *1993*. pp: 139-145.
20. Guzman H.M., Burns K.A. and Jackson J.B.C. (1994) Injury, regeneration and growth of Caribbean reef corals after a major oil spill in Panama. *Marine Ecology Progress Series* **105**: 231-241.
21. Shinn E.A. (1966) Coral growth-rate, an environmental indicator. *Journal of Paleontology* **40**(2): 233-240.
22. Lirman D. (2000) Fragmentation in the branching coral *Acropora palmata* (Lamarck): growth, survivorship, and reproduction of colonies and fragments. *Journal of Experimental Marine Biology and Ecology* **251**(1): 41-57.
23. Harriott V.J. (1998) Growth of the staghorn coral *Acropora formosa* at Houtman Abrolhos, Western Australia. *Marine Biology* **132**(2): 319-325.

24. Yap H.T. and Molina R.A. (2003) Comparison of coral growth and survival under enclosed, semi-natural conditions and in the field. *Marine Pollution Bulletin* **46**(7): 858-864.
25. Jones R.J., Kildea T. and Hoegh-Guldberg O. (1999) PAM chlorophyll fluorometry: a new in situ technique for stress assessment in scleractinian corals, used to examine the effects of cyanide from cyanide fishing. *Marine Pollution Bulletin* **38**(10): 864-874.
26. Metalpa R.R., Richard C., Allemand D. and Pagès C.F. (2006) Growth and photosynthesis of two Mediterranean corals, *Cladocora caespitosa* and *Oculina patagonica*, under normal and elevated temperatures. *The Journal of Experimental Biology* **209**: 4546-4556.
27. Coles S.L. and Jokiel P.L. (1978) Synergistic effects of temperature, salinity and light on the hermatypic coral *Montipora verrucosa*. *Marine Biology* **49**(3): 187-195.
28. Ramlan, O. & Noraswana, N. F. 2009. Distribution of Ostracods in offshore sediment around Pulau Tioman, Pahang. *Malays. Appl. Biol.* **38**(1): 11-19.
29. RCM (2008) *Pangkor survey data 2008*. Kuala Lumpur: Reef Check Malaysia.
30. Wong R.C.S., Liew M.L. and Chan C.F. (2008) Distribution of polycyclic aromatic hydrocarbons (PAHs) found in water along the northern Straits of Malacca. *Malaysian Journal of Science* **27**(3): 19-24.
31. Warner M., Lesser M. and Ralph P. (2010) Chlorophyll fluorescence in reef building corals. In Suggett D.J., Prášil O. and Borowitzka M.A. (Eds.). *Chlorophyll a Fluorescence in Aquatic Sciences: Methods and Applications* **4**: 209-222. Springer Netherlands.
32. Walz Company (1998) *Underwater Fluorometer Diving-PAM, Submersible Photosynthesis Yield Analyzer, Handbook of Operation.*
33. Davies-Colley R.J. and Smith D.G. (2001) Turbidity suspended sediment, and water clarity: a review. *Journal of the American Water Resources Association* **37**(5): 1085-1101.
34. Onset Computer Corporation (2012) *HOBO Pendant Temperature/Light Data Logger Handbook*.
35. Hubbard D.K. (1997) Reefs as dynamic systems. In Birkeland C. (Ed.) *Life and Death of Coral Reefs* pp: 43-67. International Thomson Publishing.
36. Crabbe M.J.C. and Smith D.J. (2005) Sediment impacts on growth rates of *Acropora* and *Porites* corals from fringing reefs of Sulawesi, Indonesia. *Coral Reefs* **24**(3): 437-441.
37. ISRS (2004) The effects of terrestrial runoff of sediments, nutrients and other pollutants on coral reefs. *Briefing Paper 3*, International Society for Reef Studies p. 18.
38. Anthony K.N. and Connolly S. (2004) Environmental limits to growth: physiological niche boundaries of corals along turbidity–light gradients. *Oecologia* **141**(3): 373-384.
39. Loya Y. (1976) Effects of water turbidity and sedimentation on the community structure of Puerto Rican corals. *Bulletin of Marine Science* **26**(4): 450-466.
40. Anthony K.R.N. (1999) Coral suspension feeding on fine particulate matter. *Journal of Experimental Marine Biology and Ecology* **232**(1): 85-106.

41. Anthony K.R.N. (2000) Enhanced particle-feeding capacity of corals on turbid reefs (Great Barrier Reef, Australia). *Coral Reefs* **19**(1): 59-67.
42. Ralph P.J., Gademann R., Larkum A.W.D. and Schreiber U. (1999) In situ underwater measurements of photosynthetic activity of coral zooxanthellae and other reef-dwelling dinoflagellate endosymbionts. *Marine Ecology Progress Series* **180**: 139-147.
43. West J.M. and Salm R.V. (2003) Resistance and resilience to coral bleaching: Implications for coral reef conservation and management. *Conservation Biology* **17**(4): 956-967.
44. Crabbe J. and Smith D. (2002) Comparison of two reef sites in the Wakatobi Marine National Park (SE Sulawesi, Indonesia) using digital image analysis. *Coral Reefs* **21**(3): 242-244.
45. Gladfelter E.H., Monahan R.K. and Gladfelter W.B. (1978) Growth rates of five reef-building corals in the Northeastern Caribbean. *Bulletin of Marine Science* **28** (4): 728-734.
46. Lirman D., Thyberg T., Herlan J., Hill C., Young-Lahiff C., Schopmeyer S., Huntington B., Santos R. and Drury C. (2010) Propagation of the threatened staghorn coral *Acropora cervicornis*: methods to minimize the impacts of fragment collection and maximize production. *Coral Reefs* **29**(3): 729-735.
47. Rinkevich B. (2005) Conservation of coral reefs through active restoration measures: recent approaches and last decade progress. *Environ. Sci. Technol.* **39**(12): 4333-4342.
48. Crabbe M.J.C. (2009) Scleractinian coral population size structures and growth rates indicate coral resilience on the fringing reefs of North Jamaica. *Marine Environmental Research* **67**(4–5): 189-198.
49. Madin J.S. and Connolly S.R. (2006) Ecological consequences of major hydrodynamic disturbances on coral reefs. *Nature* **444**(7118): 477-480.
50. Kaniewska P., Anthony K.N. and Hoegh-Guldberg O. (2008) Variation in colony geometry modulates internal light levels in branching corals, *Acropora humilis* and *Stylophora pistillata*. *Marine Biology* **155**(6): 649-660.
51. Garrison V. and Ward G. (2008) Storm-generated coral fragments – A viable source of transplants for reef rehabilitation. *Biological Conservation* **141**(12): 3089-3100.
52. RCM (2012) *Reef Check Malaysia Newsletter Volume 2012-01*. Kuala Lumpur: Reef Check Malaysia.
53. RCM (2011) *Pangkor status report April 2011*. Kuala Lumpur: Reef Check Malaysia.
54. Negri A., Vollhardt C., Humphrey C., Heyward A., Jones R., Eaglesham G. and Fabricius K. (2005) Effects of the herbicide diuron on the early life history stages of coral. *Marine Pollution Bulletin* **51**(1–4): 370-383.
55. Bielmyer G.K., Grosell M., Bhagooli R., Baker A.C., Langdon C., Gillette P. and Capo T.R. (2010) Differential effects of copper on three species of scleractinian corals and their algal symbionts (*Symbiodinium* spp.). *Aquatic Toxicology* **97**(2): 125-133.

Journal of Science and Technology in the tropics (2013) 9: 47-78

Microwave remote sensing for tropical vegetation

Yu Jen Lee[1], Hong Tat Ewe[2,*] and Hean Teik Chuah[2]
[1]Faculty of Engineering and Green Technology, Universiti Tunku Abdul Rahman,
Jalan Universiti, Bandar Barat, 31900 Kampar, Perak D. R., Malaysia
[2]Faculty of Engineering and Science, Universiti Tunku Abdul Rahman,
UTAR Complex, Jalan Genting Kelang, 53300 Setapak, Kuala Lumpur, Malaysia
(*Email: eweht@utar.edu.my)

Received 17-01-2013; accepted 22-03-2013

ABSTRACT A review of literature on the development and use of microwave remote sensing for vegetation in the tropics are presented. In particular, the principal areas of interest include the following:
1. Development of theoretical models to understand the electromagnetic wave-target interaction mechanisms of various types of vegetation. Such models are critical as they form the basis towards the generation of new techniques for recovering vegetation properties from electromagnetic scattering data.
2. Advancement in ground truth measurement techniques and equipment as well as collection of measurement data for future research. New methods have been developed to measure critical properties of vegetation, such as the waveguide thin sheet method for dielectric constants of leaf samples. The design of new equipment, such as scatterometers and airborne SAR systems to measure backscattering coefficients of vegetation is also important. The numerous data collected during ground truth measurements by various research groups have paved the way for the use of remote sensing technology on vegetation.
3. Image processing and classification techniques to distinguish different types of vegetation and terrain. These form the tools for large scale monitoring of crops and forests using SAR imagery. Such techniques are important, especially for the application of microwave remote sensing in disease control of crops, crop planting management and forest logging monitoring.

Keywords microwave – remote sensing – tropical – vegetation

INTRODUCTION

The use of microwave remote sensing has been advancing rapidly and has been targeted as a primary solution to earth resource monitoring and management [1]. There is currently substantial existing work being done on the use of remote sensing for various media, such as sea ice and ocean [2, 3]. In remote sensing of tropical vegetation, observations of the electromagnetic fields scattered or emitted by vegetation are used to characterize the physical

properties and conditions of the plants. Large-scale information obtained from such methods is important towards applications such as the monitoring of agricultural crops and the maintenance of tropical forests.

In the tropics, such as Asian countries, where rice is the staple food, the capability to predict the yield of paddy for a particular year may assist government agencies in the planning of food resources for its people. The use of remote sensing as a tool to enable the use of crop models for yield prediction and other applications has been recommended [4]. In terms of monitoring of large areas of crops, the use of remote sensing images with the proper image classification techniques may assist towards the control of diseases or natural hazards, thus reducing the losses of both farmers and the government, where the export of the crops may play a huge role towards the country's economy. There has been reported work on using electromagnetic data to discriminate fungal disease infestation in oil palm [5].

With the current global focus shifting towards climate change and environmental issues, the use of remote sensing towards the maintenance and monitoring of tropical forests is also being considered. Logging activities and deforestation are issues currently being tackled by several tropical countries, such as in Brazil, where the Amazon rain forests are located and also in the rain forests in Malaysia and Indonesia. Illegal logging has caused losses in millions of dollars for these countries. Such activities also contribute towards the extinction of several indigenous species of flora and fauna unique to these rain forests. Due to the vast amount of areas covered by such virgin forests, it is impossible for park rangers to cover the entire landscape to counter illegal logging or deforestation. Several efforts had been made to propose the use of remote sensing to monitor the tropical rain forests, such as the development of a monitoring system for tropical rainforest management by a joint research group from Malaysia and Japan [6].

Regardless of how remote sensing is to be applied towards vegetation, it is important to note that the development of proper theoretical models, the collection of measurement data as well as the advancement of image classification techniques are required in order to realize the potential of using remote sensing techniques for such purposes. In this paper, the collection of such methods and their principal results are reported, with focus given primarily on tropical vegetation such as paddy, oil palm and forests.

THE ORETICAL MODELING OF TROPICAL VEGETATION

In this section, several theoretical models developed to better understand the relationship between the scattering properties of tropical vegetation and microwaves are reported. In addition, models developed to model certain

parameters of tropical vegetation are also discussed. The models discussed below are but a few of the current work being done to meet this task.

Paddy

Rice plays an integral role as the staple food of most Asians and is an important agricultural crop. In China and Malaysia, the planting of paddy is important to ensure the production of sufficient food source for the people. Due to its importance, emphasis has been given to find methods to predict the yield of rice and also to monitor the growth of paddy [4]. There has been a growing interest towards the development of proper theoretical models to understand the scattering properties of paddy.

Radiative Transfer Model with DMPACT and Fresnel Corrections

There has been reported work on modeling paddy for the purpose of calculating the backscattering coefficients. Koay *et al*. [7] proposed to model paddy as an electrically dense media. In this method, paddy is modeled either as a single layer or multilayered dense discrete random medium consisting of cylindrical and needle-shaped scatterers, depending on the different growth stages (Fig. 1). In Malaysia, seeds are broadcasted randomly, resulting in fields with higher density

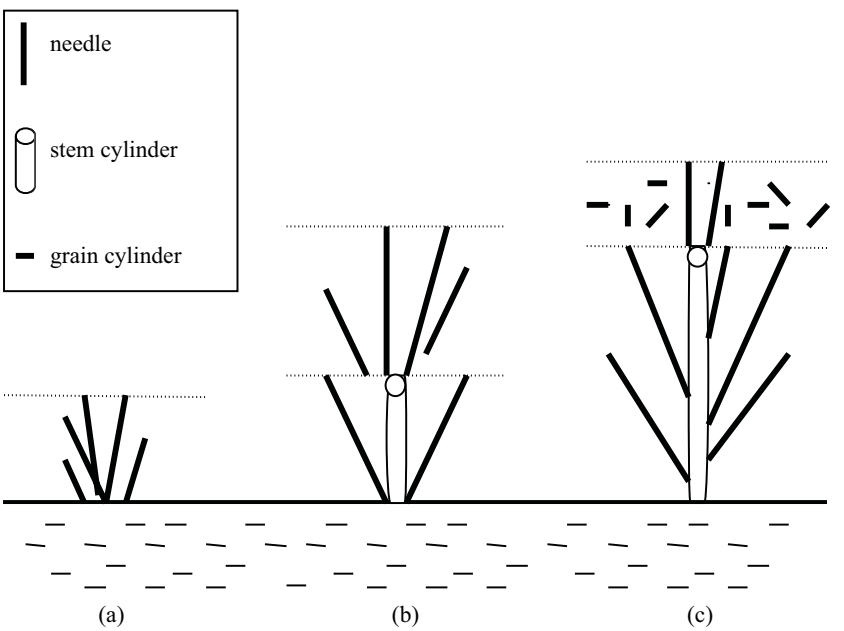

Figure 1. Variations in the model used for the computation of backscattering coefficients of paddy fields in the (a) early vegetative stage, (b) late vegetative stage, and (c) reproductive stage [7].

and randomness [7]. Due to this, previous works such as the branching model for vegetation [8] and Foldy-Lax multiple-scattering equations [9], which consider the clustering effects from the positions of scatterers, may not be accurate for the scenario in Malaysia as these methods apply more to plants that are planted in rows with space in between clusters of plants.

In order to take into account the coherent and near-field effects of the closely spaced scatterers, the Dense Medium Phase and Amplitude Correction Theory [10] is incorporated into the phase matrix. In addition, the Fresnel field effects are also considered as further improvements to the phase matrices of dense media [11-14]. The phase matrix is then applied into the Radiative Transfer equations [15, 16] and solved up to the second order [17] to consider double-volume scattering.

The theoretical model was used to calculate the backscattering coefficients of the paddy canopies, where the measured ground truth parameters such as plant geometry, dielectric constants and volume fractions were incorporated into the theoretical model equations for simulation. The ground truth measurements were carried out in Sungai Burung, Selangor, Malaysia. In addition, RADARSAT images were obtained at 24-day intervals. The specifications for the RADARSAT image were: C-band frequency of 5.3GHz, HH polarization, Fine Mode 2 with a resolution of about 8 m and an incident angle range of 39°–42°. Table 1 shows the model variation used for the different growth stages of rice crops, which corresponds to the plant age and dates of the RADARSAT image acquired.

The model was used to calculate the HH-polarized backscattering coefficients of several test fields at a frequency of 5.3GHz and at an incident angle of 41° in order for comparisons with the RADARSAT data. Figure 2 shows the comparison between the model prediction and the actual backscattering coefficients calculated from the RADARSAT image for different stages of growth.

Table 1. Variations in the model for different growth stages [7].

Date	Test Field	Age (days)	Model Variation
20-09-2004	1	27	Early vegetative
	4	26	
	5	29	
	6	21	
14-10-2004	1	51	Late vegetative
	4	50	
	5	53	
	6	45	
06-11-2004	1	75	Early reproduction
	4	74	
	5	77	
	6	69	

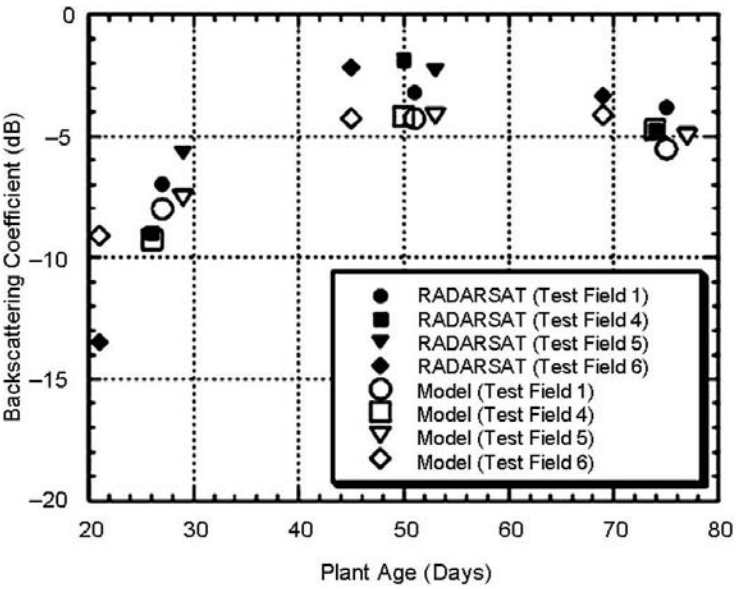

Figure 2. Comparisons of theoretical and measured HH-polarized backscattering coefficients at different stages of growth [7].

It was observed that the total backscattering coefficient increased during the vegetative stages of the paddy plants as the plants grew taller and denser, but decreased slightly at the reproductive stage, which might be due to halted growth of plants and the dying off of smaller plants. The results show good matching in general, but errors of about 2 dB were noticed at the age of 50 days. Such errors were expected since the ground truth measurements were not exact statistical representations of actual fields and might not be accurate. Another possible reason could be the needle shape used to model the leaves, which might not be suitable as some leaves could be wider in dimension.

Comparisons between the dense medium model and the Monte Carlo simulations were also carried out for VV-polarized backscattering coefficients based on parameters given in [18]. Figure 3 shows that there was not much difference in the results when the plants had a lower biomass when they were young. However, as the plants grew and the biomass increased, the dense medium model gave a better match with the ERS-1 data obtained at Samarang [18] and Akita [19] due to the higher density of the canopy.

In summary, a theoretical model developed for paddy fields using Radiative Transfer theory was proposed [7] with consideration given to the coherent and near-field effects of closely packed scatterers by incorporating the DM-PACT and Fresnel correction terms in the phase matrix of the paddy canopy. Multiple volume scattering was also considered by incorporating second-order solutions of the Radiative Transfer theory. Utilizing ground truth measurements obtained

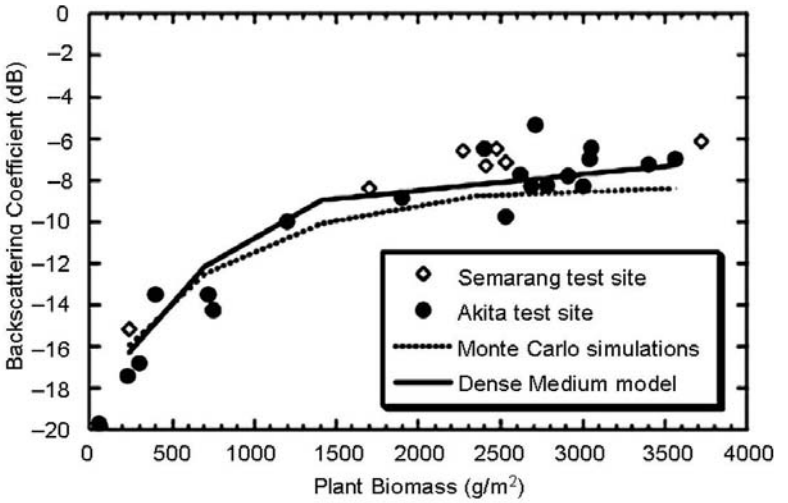

Figure 3. Comparisons of the backscattering coefficients obtained through the dense medium model, Monte Carlo simulations, and ERS-1 data with respect to the plant biomass [7].

for an entire season at Sungai Burung, Selangor, Malayia, a theoretical analysis using the model was carried out (detailed discussion of the analysis can be found in [7]). It was found that multiple-volume scattering effects are important in the calculation of cross-polarized backscattering coefficients and will be critical for applications involving polarimetric data. Coherent effects need to be considered at lower frequencies while Fresnel corrections are more important at higher frequencies. The simulated results compared with RADARSAT images and the Monte Carlo simulations showed promising results. A suggestion to improve the model is to use elliptical disk-shaped scatterers in the phase matrix [20].

Vector Radiative Transfer Model

There are also other backscattering models utilizing Radiative Transfer theory. Ma *et al*. [21] proposed a first-order microwave backscattering model for rice canopy, where the rice canopy is characterized as a uniform layer containing leaves and stems, while the spike of rice is omitted. The model is based on the Vector Radiative Transfer theory [22] and adapts the MIMICS backscattering model originally developed for forest canopy. The backscattering coefficient of the various polarizations was calculated as:

$$\sigma_{vv}^{0} = 4\pi\mu_0[T]_{11}, \sigma_{hh}^{0} = 4\pi\mu_0[T]_{22}$$
$$\sigma_{hv}^{0} = 4\pi\mu_0[T]_{21}, \sigma_{vh}^{0} = 4\pi\mu_0[T]_{12} \quad (1)$$

Figure 4 shows the variations of the rice backscattering with the date at C-band, with the incidence angle at 23°. 3D figures were then plotted with reference to the dates (Fig. 4) to illustrate that the backscattering coefficient depends on the incidence angle and varies with the growth for L-band, C-band and X-band. The results obtained were consistent with work reported in [18] and [19]. The plot for C-band are shown in Figure 5.

Single Layer Radiative Transfer Model

Shao *et al*. [23] successfully predicted the radar backscatter behaviour of rice by using an established Radiative Transfer model for vegetation canopies developed by Sun *et al*. [24] on rice. The study focused on the temporal characteristics of rice backscatter as a function of polarization at C-band. This study was carried out in the Zhaoqing test site located in Guangdong Province in Southern China. The multi-temporal RADARSAT image set comprised of 7 scenes acquired in

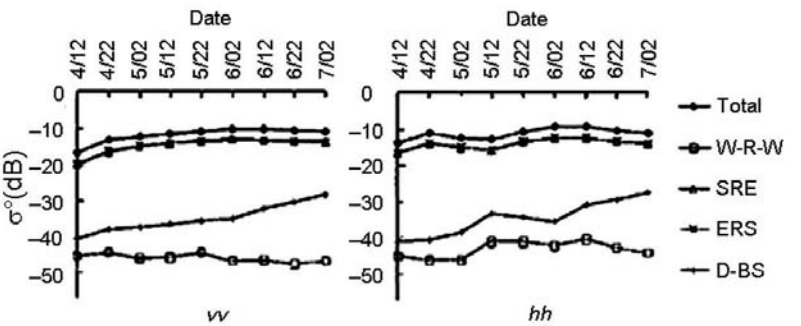

Figure 4. The variations of the rice backscattering coefficient with date (C-band, incidence angle = 23°) [21].

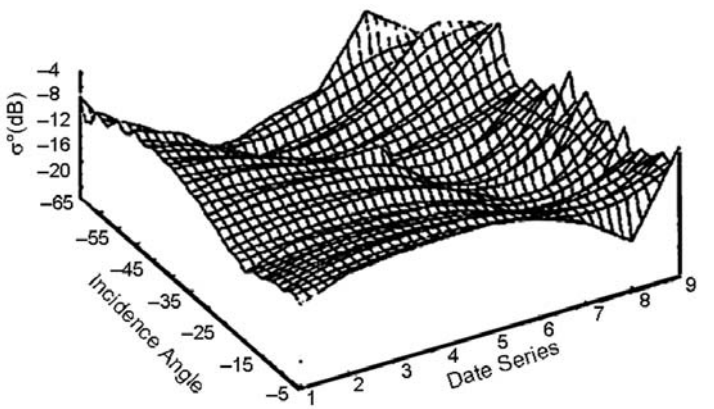

Figure 5. C-band HH polarization [21].

Standard Mode from April to July, 1997. Rice physical measurements were carried out during the period of the RADARSAT acquisition. The fresh biomass of rice was determined by:

$$M = [1000/a \times 1000/b] \times W_f \times N \qquad (2)$$

where a is the row spacing; b, the line spacing; W_f, the fresh weight of each rice seedling; and N, the numbers of rice seedling of each cluster. The dielectric of rice was calculated from the gravimetric water content using the empirical Dual-dispersion model [25].

The model was used to generate backscatter coefficients for all polarizations. It was found that for HH polarization, the generated data managed to fit the few RADARSAT observations reasonably well (Fig. 6).

Further analysis of the generated backscatter coefficients shows that at a 45° incidence angle, crown backscatter at HH and HV polarization increases as the rice grows. However, at VV polarization the crown backscatter increases at the early stage of the rice growth cycle and then stays relatively constant for the rest of the rice growth cycle, which corresponds to results reported in [18]. Further research is needed to fully utilize the model's capabilities.

Coherent Electromagnetic Model

Other works on theoretical modeling of rice include work done by Fortuny-Guasch *et al*. [26] and Ma *et al*. [27]. In [26], a physics-based coherent electromagnetic model tailored for the computation of radar backscatter from rice was developed. The model considers the rice as an arrangement of plants over a flooded soil, where the plants are modeled as clusters of dielectric cylinders. The results show that the co-polar backscattering coefficients obtained

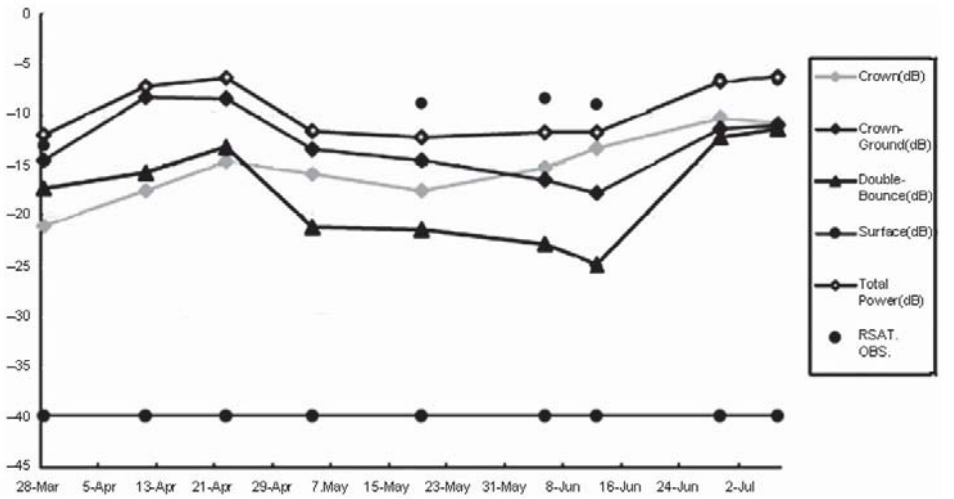

Figure 6. Comparing model results with RADARSAT observations in 1997 [23].

by the model are similar to the measured ones, but the cross-polar scattering obtained is much lower. Future consideration into multiple scattering between stems was suggested as an improvement to the current model.

Radiative Transfer Model with Lindenmayer System

In [27], the employment of the Lindenmayer system (L-system) [28] and computer graphics technique to describe the realistic structure of the rice crops was studied. On the basis of such method, according to the physical interaction principle between electromagnetic wave and vegetation, the intensity of scattered field of each scatterer was calculated. By coherent addition of the individual scattered field of each scatterer, the total backscattered field of the crop canopy can be obtained and the backscattering coefficients can be calculated. The simulation results were compared with the measurement data obtained via scatterometer. The results show that the predication of backscatter is roughly identical to the measurement, especially when the incidence angle is between 20° and 50°.

Studies have also been conducted on relating physical properties of the rice to the microwave backscatter. Using the proper algorithms and models, the variations in the backscatter are compared with variations in certain parameters in the rice.

Modeling of Rice Parameters

The modeling of dielectric microwave properties of rice using the Debye-Cole dual-dispersion model of vegetation was studied in [29]. Results show that the dielectric constant of rice varies at different growth stages. The dielectric constant increases during the transplant to seedling developing period but decreases after that. On the other hand, microwave frequency, gravimetric moisture content of rice, temperature and density of dry rice canopy have an influence on dielectric constant. In the study, salinity had no effect on the dielectric constant.

The mapping of rice biomass was done using ALOS/PALSAR imagery [30]. By integrating a rice canopy scattering model [31], the spatial distribution of paddy rice biomass was simulated. Plant height and density were the two most determinant biophysical parameters related to rice biomass, which could be retrieved with an error of less than 6 cm and 30/m^2, respectively. Thus, the biomass could be estimated with an adjusted residual of 200 g/m^2. The results indicate that the designed approach was useful to quantitatively estimate the carbon absorption from the atmosphere during the growing season of rice and demonstrated the potentials of using ALOS/PALSAR data for the mapping of rice biomass using the microwave canopy scatter model.

Another important parameter relating to microwave backscatter is the leaf area index (LAI). Stephen *et al*. [32] demonstrated this by modeling the flooded rice field as a single layer of discrete scatterers over a reflecting surface using the Distorted Born Approximation. At C-band, the VV polarization radar backscatter

decreased with increasing LAI over the observed range of LAI. Further investigations using the simple model showed that the decrease was related to the domination of direct-reflected backscatter over the direct component. Model calculations suggested that at very low LAI the radar backscatter should increase with LAI.

Inoue *et al*. [33] observed unique interactions between each of the microwave backscatter coefficients at all combinations of five frequencies (Ka, Ku, X, C and L), all polarizations (HH, VH, HV and VV) and four incident angles (25°, 35°, 45° and 55°) and vegetation variables such as leaf index area (LAI), biomass and grain yield. The study revealed that the realistic cropping condition of rice would allow further quantitative insight on the interaction of backscatter with vegetation.

Oil Palm

Besides paddy, oil palm is another commodity that is important in the tropics. Palm oil is viewed as a potential biofuel source in the future as the amount of fossil fuel dwindles. It has also found uses as key ingredients in a variety of areas, such as cooking oil, soaps and glycerol. Countries such as Indonesia, Malaysia, Nigeria and Colombia are but a few of the tropical countries producing palm oil with the growth of oil palm plantations.

3D Model with Radiative Transfer Theory

Izzawati *et al*. [34] adapted a 3D radar backscatter model originally designed for forest canopies [35] to simulate high resolution images of polarimetric radar backscatter of oil palm plantations at different growth stages. The main purpose was to examine the relationships between the backscatter and texture and crop status in order to invert the latter from space borne SAR data. The individual crowns were modeled as hemispheres and distributed in a triangular pattern found in oil palm plantations. Polarimetric radar backscatter was then simulated for C and L band at high spatial resolution for a range of growth stages and LAI.

The original 3D radar backscatter matter was based on the Radiative Transfer equation for a forest canopy comprising a crown layer, trunk layer and rough-surface ground boundary. For the study, steps were taken to ensure the production of reliable oil palm plantation stands at different growth stages to be used as input in the model. Simulations were then carried out on the oil palm plantation using the theoretical model at C and L band.

Multipolarized high resolution images (0.5 m) were simulated using the model at years 2.5, 6.5 and 8.5 for C-band and at years 2.5, 4.5 and 6.5 for L-band (Fig. 7, 8). The estimation of the mean radar backscatter of C and L bands at HH, HV and VV polarizations were also completed. A texture analysis was also done using directional semivariograms. Early modeling results indicate

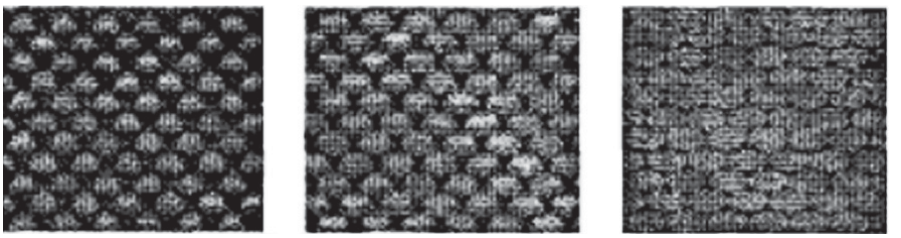

Figure 7. C-band simulation at age 2.5, 6.5 and 8.5 years [34].

Figure 8. L-band simulation at age 2.5, 4.5, and 6.5 years [34].

the potential of using mean backscatter and semivariance measures to discriminate oil palm stand age.

Tropical Forest

There has been a multitude of reported work focusing on the modeling of vegetation in general [8, 11-13, 17, 35, 36]. Some of these models actually form the basis for the model developed for paddy and oil palm. Many of these models were previously validated on temperate climate forests, such as Boreal or Cypress forests. In this section, modeling done and validated on tropical forests is discussed.

Hybrid Coherent Scattering Model

Thirion *et al*. [37] looked into several earlier models and concluded that there is a need to study the different scattering mechanisms involved in the forest by means of a fully coherent scattering model (COSMO). They proposed a new hybrid model derived from the RVoG model. Retrieval studies indicated that the model seems to be more adapted to the P-band. COSMO is a coherent descriptive model that is applied to radiometry, interferometry and polarimetry. In the paper, the model was used to simulate SAR data for Mangrove (tropical) and Nezer (temperate) forests for P-band and L-band. The comparisons between the simulations and the real SAR data were satisfactory in radiometry for both types of vegetation. The model also showed good ability to simulate the interferometric data and polarimetric behaviour of the vegetation mentioned.

Multilayer Radiative Transfer Model

The use of multilayer models to model vegetation has also been proposed [11, 17]. Ewe *et al*. [11] treated vegetation as an electrically dense media. Utilizing the Radiative Transfer theory, the array phase correction factor was incorporated into the phase matrices of the nonspherical scatterers to take into account the coherent effect between scatterers. In addition, the amplitude and Fresnel phase corrections were also included when the Fresnel factor was larger than p/8. The improved phase matrix was then included into the Radiative transfer formulation. Finally this formulation was solved iteratively up to the second order to incorporate the multilayer effects. It was found that the measurement results for Japanese cypress and boreal forest with multifrequency and multipolarization data showed good agreement with the theoretical predictions from the model. There is huge potential for the model to be used to model for tropical dense forest.

Karam *et al*. [17] came up with a two layer scattering model for trees and tested it on both coniferous and deciduous trees. In the model, the two layers are the crown layer and trunk layer above an irregular surface. Deciduous leaves, which are quite common in tropical trees, are modeled as randomly oriented circular discs. The advantages for this model is that it accounts for the first and second order scattering within the canopy, fully accounts for the surface roughness in the canopy-soil interaction terms, allows many branch sizes and orientation distributions, and finally is valid over a wide frequency range for both deciduous and coniferous vegetation.

Validation was carried out by applying the model to walnut and cypress trees. A comparison between the backscattering measurements and the model predictions was done. Additionally, the effects of frequency, second order interaction and surface roughness effects were studied. It was found that in order to obtain good matching between calculated and simulated backscattering coefficients, the branch size distribution is important. The model discretized branch size distribution into four sizes. Next, small branches and leaves generally contribute to the backscattering coefficients at X-band. For deciduous trees, cross polarization at X-band is dominated by stems rather than leaves. Lastly, soil moisture and soil roughness are more important for HH polarization as they influence the trunk-soil interaction contribution to the backscattering coefficients.

GROUND TRUTH MEASUREMENT OF TROPICAL VEGETATION

The development of theoretical models is important to understand the physics and interaction between electromagnetic waves and vegetation. The results from these studies also aid in the development and design of proper ground truth measurement systems.

Development of Measurement Tools

One important aspect in the study of remote sensing is the design of measurement tools to perform ground truth measurements.

Ground based scatterometers

Ground based scatterometer systems are popular methods for the collection of backscattering data from agriculture vegetation such as paddy and oil palm. Due to its importance, the development of ground based radar is as important as airborne SAR. Koo *et al*. [38] reported the development of a ground based radar for scattering measurements operating at C-band. Constructed from a combination of commercially available components and in-house fabricated circuitry, the system has full polarimetric capability for determining the complete backscattering matrix of a natural target. A microwave sensor was constructed and installed onto a boom truck (Fig. 9). Designed for short-range operations, a frequency-modulated (FM-CW) configuration was employed for the scatterometer system. Table 2 summarizes the system's specifications.

Figure 9. A photograph of the scatterometer system.

Table 2. Specifications of ground based scatterometer [38].

System Parameter	Specification
System Configuration	
Type	FM-CW
Operating frequency, f_c	6 GHz (C-band)
Operating wavelength, λ	5 cm
Sweep Bandwidth, B	400 MHz
Modulating frequency, f_m	60 Hz
Polarization	HH, VV, HV, VH
Polarization isolation	35 dB
Antenna gain, G	35 dB
Antenna 3 dB beamwidth, β	3°
Best possible range resolution, v_R	0.375 m
Platform	Boom truck
Platform height, h	25 m (vertical)
Measurement Capability	
Transmitter power, P_t	10 dBm
Received power, P_r	–15 dBm to –92 dBm
$\sigma°$ Dynamic range	+20 dB to –40 dB
Measurement range, R	20 m to 100 m
Incident angle coverage, θ	0° – 70°
Minimum signal-to-noise ratio, SNR	10 dB
Effective range resolution, ΔR	(~1.8 m at θ = 45°;4.5 m at θ = 60°)

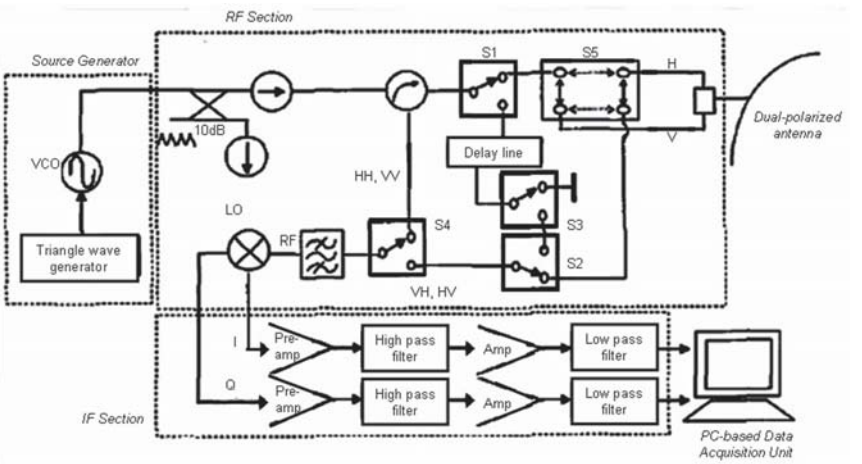

Figure 10. The system block diagram [38].

Figure 10 illustrates the simplified system block diagram, where the main sections are the RF section, the antenna, the IF section and the data acquisition unit. The system was tested in a low reflection outdoor environment [38]. The results from the measurements in the tests were compared with the theoretical values to evaluate the measurement accuracy.

Figure 11 shows one of the RCS measurement carried out. In general, it was observed that the measured scattering matrices had good agreement with

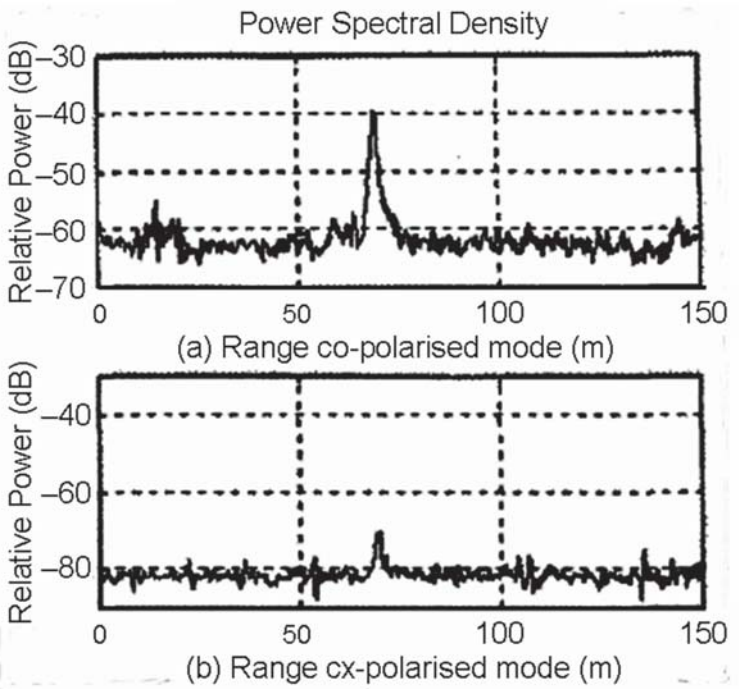

Figure 11. The measured power spectra of an 8" trihedral corner reflector [38].

the theory and the measurement accuracy was within ±1.5 dB in magnitude and ±10° in phase. The scatterometer system has been used to conduct in-situ backscattering measurements of tropical crops.

There has also been a multitude of other developed ground based scatterometers utilized for the remote sensing of tropical vegetation, in particular rice crops. In [39, 40], an FM-CW scatterometer with four parabolic antenna (L, S, C, X) configurations was designed and utilized to collect microwave backscatter signatures of paddy over the entire rice-growing season. An X-band scatterometer system named POSTECH Polarimetric Scatterometer (POPOS) was designed and implemented by *Kim et al*. [41] to obtain radar backscattering measurements of rice crops over the whole period of rice growth at three polarization combinations.

The experience and success in the design and implementation of various types of ground based scatterometers gives rise to the confidence to develop airborne SAR systems.

Airborne SAR

There has been reported work on the development of airborne synthetic aperture radars. Koo *et al*. [42] developed the Malaysian Airborne Synthetic Aperture

Radar (MASAR) for the purpose of earth resource monitoring, such as paddy fields, oil palm and soil surface. This SAR system is a C-band, single polarization, linear FM radar. The preparatory studies on the conceptual design of the microwave system were presented by Chan *et al*. [43]. The SAR system is capable of operating at moderate altitudes with low transmit power and small swath width.

The first step towards the design of the MASAR system is the model simulation carried out to select design parameters crucial towards the optimization of the hardware and software system performance. This was done by developing a modular-based simulator consisting of several independent modules sharing a pool of data files (Fig. 12) and implementing it using Matlab software. The design parameters were then iteratively selected and the results were evaluated using the SAR simulator. Table 3 presents the selected system parameters for the MASAR system.

The functional block diagram for the MASAR system (Fig. 13) consists of a microstrip antenna, a radar electronics subsystem and a data acquisition system [for details, see [42]). A prototype RF transceiver for both ranged detection and radar cross section (RCS) measurement was also developed and verified in field experiments [44]. Finally, the algorithm for the MASAR image formation was developed based on the parallel implementation of the wavefront reconstruction theory, known as the range-stacking algorithm. The range-stacking algorithm does not require interpolation and does not suffer from truncation errors.

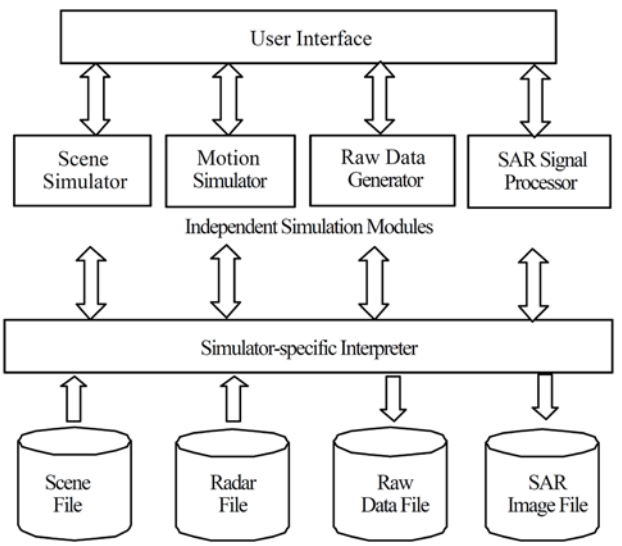

Figure 12. Block diagram of a modular-based SAR simulator [42].

Table 3. The MASAR specifications [42].

System Parameter	Specification
Mode of operation	Stripmap
Operating frequency, f_c	5.3 GHz (C-band)
Bandwidth, B	20 MHz
Chirp pulse duration, τ_p	20μs
Pulse repetition frequency	1000 HZ
Transmitter peak power, P_t	100 W
Polarization	Linear, VV
Antenna gain, G	>18 dBi
Elevation beamwidth, β_{el}	24°
Azimuth beamwidth, β_{az}	3°
Synthetic aperture length	~200 m
ADC sampling frequency	100 MHz
ADC quantization	12-bit
Data rate, d	100 Mbps
Recorder capacity	2 × 160 GB, SATA
Data take duration, T_d	>5 hours
σ° dynamic range	0 dB to –30 dB
Signal-to-noise ratio, SNR	>10 dB
Best slant range resolution	7.5 m
Best azimuth resolution, ρ_a	7.5 m (2-looks)
Incident angle, θ	50°
Swath width, W	~8 km
Platform height, h	7500 m
Nominal platform speed, v_0	100 m/s
Operating platform	Pressurized aircraft

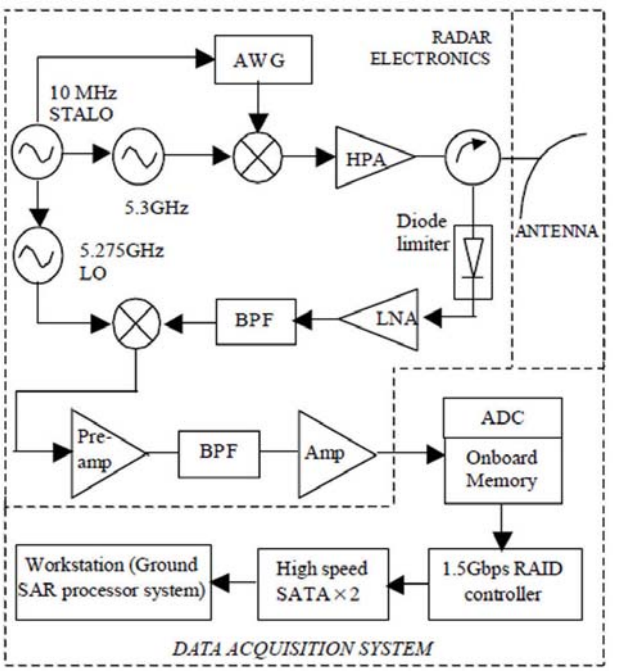

Figure 13. System block diagram of MASAR [42].

The MASAR project is an on-going activity and work is being done to mount the SAR system onto an unmanned aerial vehicle for flight commissioning and actual field measurements.

Anechoic Chamber

The potential to conduct controlled laboratory experiments to perform various electromagnetic field measurements has led to the design and construction of an anechoic chamber at Multimedia University, Cyberjaya, Malaysia [45]. While yet to be implemented on tropical vegetation, there is huge potential to utilize this facility in the future to conduct such experiments in a controlled environment. In order to design a good anechoic chamber, Chung *et al*. [46] performed the necessary modeling of anechoic chamber using a variant of the beam tracing technique to study the normalized site attenuation (NSA) performance of the anechoic chamber. In addition, work was also done to develop a model for the pyramidal RF absorber with pyramid length shorter than a quarter wavelength and poor reflectivity performance [47].

The structure of the anechoic chamber is a quarter-section geodesic dome, with a 12 foot radius and raised three feet above the floor [48]. Figure 14 shows the floor plan of the anechoic chamber, which can be used for monostatic and bistatic radar cross section measurements. Figure 15 shows the measurement system configuration, where two six-pole RF switches select the transmitting antenna and the receiving antenna to be used in a particular measurement. The main component of the measurement system is the Wiltron 360B Vector Network Analyzer (VNA).

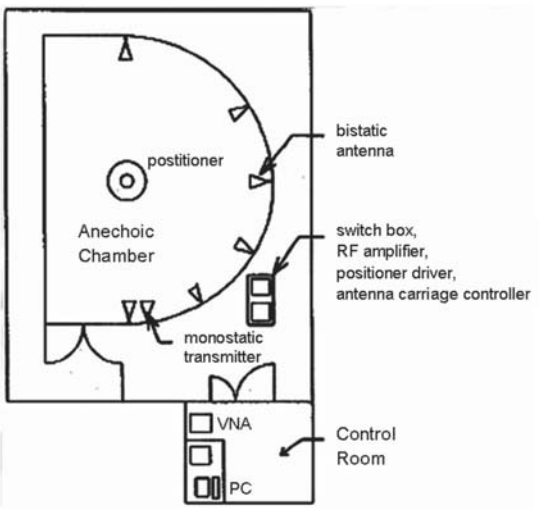

Figure 14. The anechoic chamber floor plan [48].

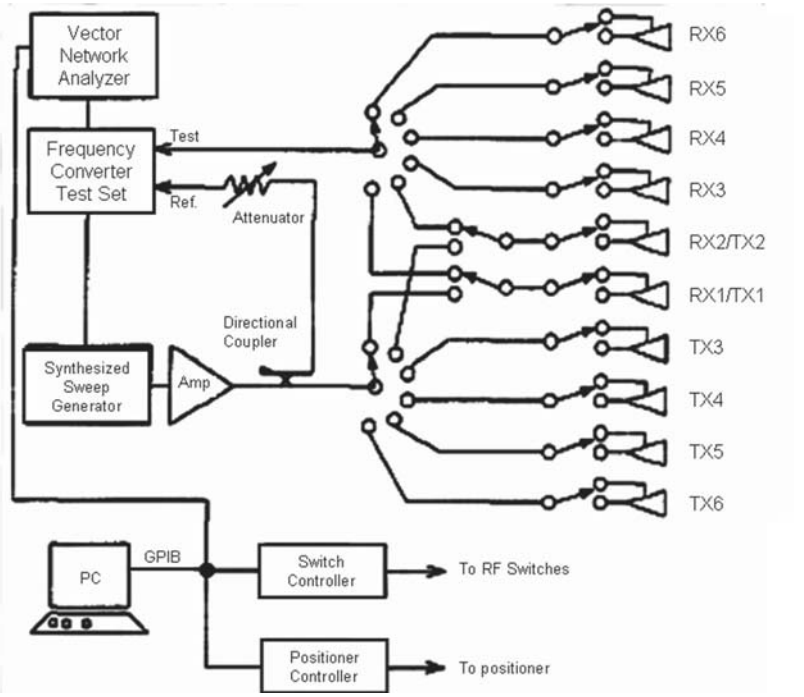

Figure 15. The measurement-system configuration [48].

The calibration of the measurement system was then performed to remove systematic errors due to the frequency response of the hardware, source-impedance matching, continuity of the transmission line and residual echo from the chamber background. The equation for the scattering cross section is written as:

$$\sigma_{A(t\,\mathrm{arg}\,et)} = \frac{S_{11M(t\,\mathrm{arg}\,et)} - E_D}{E_R} \qquad (3)$$

where s_A is the actual scattering cross section; E_D, the directivity error; S_{11M}, the measured reflection coefficient; and $E_{R,}$ the reflection tracking error. The measurement accuracy of the system was then investigated. Figure 16 shows the frequency-domain response. It was found that the measurement error was within ±0.5 dB across the frequency range from 2 to 16 GHz.

Future work with anechoic chamber includes scattering measurement on young tropical trees such as rubber and oil palm.

Moisture sensors

Moisture sensors are important measurement tools as they can provide parameter inputs to the developed theoretical models. The data collected from these sensors are also useful to verify the results obtained from theoretical models as well. The

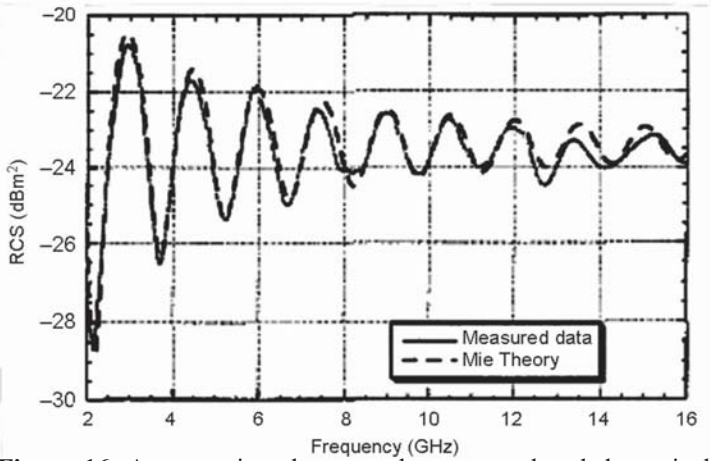

Figure 16. A comparison between the measured and theoretical frequency behaviour of the monostatic RCS of a 3" sphere after time-domain gating [48].

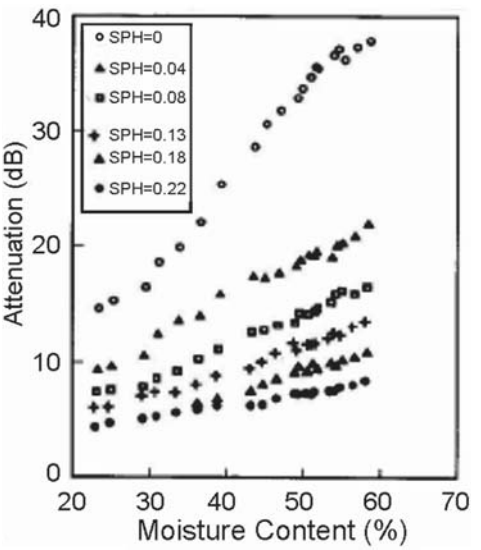

Figure 17. Variation of attenuation or insertion loss with moisture content for microstrip sensors [49].

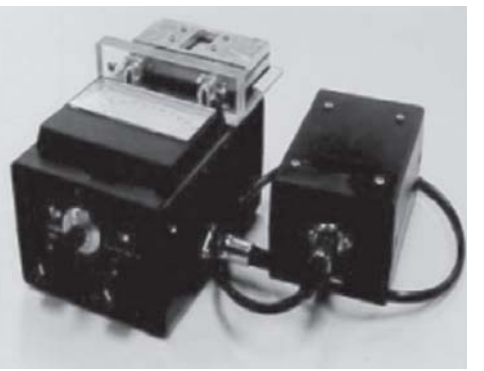

Figure 18. A prototype of ripeness meter for oil palm fruit [49].

Figure 19. A prototype model for dual-frequency microwave liquid moisture meter [49].

dielectric properties of a non-magnetic material play an important role in the interaction with electromagnetic waves. Understanding this importance, Khalid *et al*. [49] proposed the development of planar microwave moisture sensors. In the study, the close relationship between moisture content and dielectric properties for both hevea rubber latex and oil palm fruits were investigated.

The attenuation of the microstrip sensor against the moisture content for hevea latex and for various thickness of protective layer is shown in Figure 17. The deviation of the test result of the moisture parameter is less than 1% compared to that obtained by Standard Gravimetric method. The microstrip sensor was integrated into the designed ripeness indicator prototype for oil palm fruits (Fig. 18). The detected current from the meter is related to the moisture content of mashed mesocarp and finally the stage of the ripeness can be determined.

A dual frequency sensor was also developed to measure moisture content of the rubber latex. The design is based on the measurement of magnitudes of the near field reflection at two frequencies in the X-band, 8.48 and 10.69 GHz. The design also replaces the conventional open horn antenna with microstrip radiating patches. This construction makes the sensor more versatile and compact and removes the temperature effect on moisture content measurements without involving phase measurement. A calibration equation was then found that instantly gives moisture content of the samples using the developed sensors. The system was tested using rubber latex and had predicted moisture content with a standard error of less than ± 0.4% compared to standard oven drying techniques and a mean error of less than ±1.3% in the temperature range of 25°C to 60°C. The prototype version of the dual-frequency moisture meter is shown in Figure 19. Future consideration for this work is to expand the method to construct moisture sensors for other products such as palm oil.

The development of various ground truth measurement systems and sensors has allowed researchers to conduct year long measurements at various sites.

Measurement Data Collection

The collection of various parameters from tropical vegetation is essential towards the validation of theoretical models and image classification techniques for microwave remote sensing and also for future references. Most parameters can be obtained directly through simple measurements, such as plant height, trunk diameter and circumference, leaf length, etc. Other parameters however may require the use of equations from various theoretical models to calculate. As such, the development of such models is important as they indirectly contribute towards the application of remote sensing for earth terrain monitoring. In addition, there are also plenty of measurement data collected via different techniques on tropical vegetation. Some of these measurements were carried out for the entire growth cycle of the plants and may provide crucial data for the remote sensing of such media.

Dielectric constant is an important biophysical parameter that plays a crucial role in the validation of theoretical models and the development of yield prediction models for tropical crops. Chuah *et al*. [50] explored the accuracy of two theoretical models that were used to estimate the dielectric constants of leaves from two tropical crops (rubber and oil palm) as a function of moisture content at X-band. The models being studied were the simple dielectric theory by Fung and Fung [51] and the dual-dispersion model by Ulaby and El-Rayes [52]. Utilizing the waveguide thin sheet technique to measure the dielectric constant of the leaves, they were able to successfully evaluate the performance of both models. It was found that the dual-dispersion model gave a more accurate estimation of the dielectric constants and thus confirmed its applicability to the leaves of rubber and oil palm in future research work.

Other parameters important towards yield prediction models and growth assessment are above ground biomass (AGB) and stem volume. Previous works measured oil palm biomass and stem volume from mature oil palm by destructive sampling which involved weighing all the major components of biomass and stem volume for different ages [53]. These studies extrapolated the data from the destructive measurements on a few palms from each age group, but the procedure might be underestimated due to restricted sampling areas. In addition, the method is tedious and time consuming.

Asari *et al*. [54] proposed the measurement of the parameters using the non-destructive sampling as a preliminary study towards the development of a prediction model for the estimation of oil palm above ground biomass and stem volume using remote sensing data. The main aim of the study was to estimate the two parameters at different ages using the non-destructive method and to study the relationship between oil palm biomass and several parameters such as crown width, height, the diameter of breast height, length and depth of petiole of oil palm stand. The study found that the trunk biomass contributed a major portion of the oil palm biomass, about 86 to 95% from the total AGB. The study also discovered that the age of the oil palm was directly correlated to above ground biomass, while stem volume was inversely correlated with the age of oil palm. A full scale study combining the ground information and remote sensing is being conducted.

Vegetation water content (VWC) plays a significant role in the retrieval of soil moisture from microwave remote sensing and also in forest and agricultural studies such as drought assessment and yield prediction. Kim *et al*. [55] reported that previous studies analyzed the relationship between NDVI and VWC and developed techniques to estimate VWC and other biophysical variables. They went a step further and examined the relationship between polarimetric radar data, VWC, LAI and normalized difference vegetation index (NDVI) using soybean and rice, focusing on the use of radar vegetation index (RVI) to estimate

VWC. In order to perform the study, the backscattering coefficients for L-, C- and X-bands, vegetation indices (RVI, NDVI and LAI) and VWC were observed over rice and soybean growth cycles. Retrieval equations were then developed for estimating VWC using the RVI of both crops. The study concluded that L-band RVI was well correlated with VWC, LAI and NDVI compared to C- and X-band and thus achieved the most accurate VWC retrievals. It should be noted however, that the investigation only focused on a 40° single incidence angle observing system since this study would be employed on the NASA Soil Moisture Active Passive satellite (SMAP) in the future. As such further studies may explore the effects of the incidence and azimuth angles.

The measurement of radar backscatter data from paddy, especially over the entire growth cycle is also important towards the development of yield prediction models via remote sensing. There is a substantial amount of reported work on the radar measurements microwave backscattering coefficients of rice plants [39-41, 56]. In these papers, the measurements of the rice plants were carried out using constructed ground based scatterometers over multifrequency and multipolarization covering an entire rice growing season. The locations of the measurements covered areas in Japan, China and Korea. In addition, measurement of other parameters such as LAI, biomass, etc. were also performed on the paddy. While the earlier works performed radar measurements using ground based scatterometers, the attempts to use space borne satellites for such measurements are few. Kurosu *et al*. [19] presented their measurements on monitoring rice crop growth from space using the European Remote Sensing satellite 1 (ERS-1). The SAR measurements were performed at the rice fields of Akita Prefectural College of Agriculture covering two growing seasons in 1992 and 1993 and were the first attempt to monitor rice crop growth from space covering all growth stages.

Tropical forest biomass estimation is important for global research. Such correlation analysis forms the base for developing models and techniques to estimate tropical forest biomass from remote sensing data. Yang *et al*. [57] utilized LANDSAT TM data and the biomass data collected from main tropical forest vegetation types in Xishuangbanna, China for studying the correlations between the biomass of vegetation types. The study found that the relationships between the biomass of monsoon tropical forest and LANDSAT TM6 and TM7 were the strongest. TM6 was positively and significantly (at 95% level of confidence) related to forest biomass while TM7 was inversely and significantly (at 95% level of confidence) related to forest biomass. Lastly, the LANDSAT TM was observed to be not significantly (at 95% level of confidence) related to the forest biomass for both the mountainous tropical forest and the seasonal ever-green broadleaf forest.

IMAGE PROCESSING TECHNIQUES FOR THE REMOTE SENSING OF TROPICAL VEGETATION

Remote sensing has proved to be an extremely convenient method to monitor large areas of agriculture crops or forests. The use of SAR images from airborne or space borne radar allows the coverage of large areas and provides huge amount of information. Image processing thus plays a crucial role, as it is important for researchers to be able to differentiate between areas of interest from other landscape captured within the image. The proper image processing tool will be required in order to correctly analyze the image and highlight the areas of interest.

Chuah *et al.* [1] reported the use of fractal dimension of images as an additional input to a neural network classifier to classify different areas of interest. Preliminary results showed that fractal analysis was useful towards the classification of sea, urban, forested and paddy areas. Ouchi *et al*. [58] explored the comparison between the use of optical and radar images on the classification of mangrove, virgin forests and oil palm plantation with the ground truth data collected from the field survey. Visible and infrared images were acquired using MOS-1b, while SAR images from JERS-1 at L-band and ERS-2 at C-band were also obtained.

The optical images were capable of classifying deforestation areas, but applications to mangrove forests were limited. SAR images performed better and were capable of differentiating the mangrove from virgin forests [58]. It was concluded that due to the longer penetration depth of L-band, the JERS-1 performed better than the ERS-2, even though both the mangrove and virgin forests had similar biomass well above the saturation range of the L-band RCS. The top image in Figure 20 shows the 3-look image of the Sematan test site in 1993, with the difference in intensity between the mangrove and neighbouring virgin forests about 6dB, making it possible to extract the mangrove area. The classified image is shown in the middle of Figure 24 and shows good agreement with the OS (Ordnance Survey) map at the bottom. The reason in the difference

Figure 20. JERS-1 SAR image of the Sematan mangrove and surrounding forests (left), classified image (centre) and OS (Ordnance Survey) map (right) [58].

in intensity is associated with whether the ground is covered by water or undergrowth, which is supported by the difference in image intensity between dry and wet seasons. Lastly, the study also showed that the ability to monitor palm oil trees is limited to the early stages of plantation.

The use of SAR images in L-band and C-band for the purpose of rice mapping and monitoring has been carried out by various research groups. Zhao *et al*. [59] carried out a study on rice monitoring using ENVISAT ASAR data over a period of three years in Jiangsu Province of China. The study showed that multi-temporal and multi-polarization radar data have great advantages in rice mapping and also parameter inversion. A practical scheme for rice yield estimation has been put forward, but further studies will need to be performed to improve its accuracy.

Yamada [60] investigated the relations between ground features and mathematical morphology using JERS-1 data during flooding time in paddy areas. The study was to improve on classification of flood areas from paddy fields or floating rice growing regions. Applying computational mathematical morphology to flood extent recognition showed promising results, with improved differentiation between paddy field areas, river courses and irrigation canals and human activity areas.

The classification of rice and sugarcane from other cover types such as water, urban areas, bush and scrubs using ERS-1 and JERS-1 satellites in Kanchanaburi, Thailand was explored [61]. Using qualitative and quantitative measures to investigate the separability of different cover types, results showed that the use of at least two appropriately timed imaging dates during the growing season was sufficient for rice field inventory. However, the study also showed difficulty in discriminating sugarcane from shrubs using the SAR images.

Several projects using image classification and mapping on tropical forests were also carried out. A joint research between Malaysia and Japan developed a monitoring system for tropical rain forest management [6]. The study was divided into three main areas: characteristics of high resolution remote sensing sensors such as LANDSAT TM, SPOT HRV and MOS-1, the study of global forest environment using NOAA AVHRR, where NOAA GAC data were used to estimate the surface temperature and evapotranspiration of Peninsula Malaysia, and zoning technology using a combination of a GIS system with remote sensing data processing system for managing tropical forest environment. Another similar project, where remote sensing was used to extract environmental information of a tropical mountainous forest was carried out in a National Park in Vietnam [62]. Parameters crucial towards the management of the mountainous forest, such as wetness, groundwater conditions, geological structure and land cover changes were successfully extracted by application of

remote sensing and GIS analysis. The Central Africa Mosaic project (CAMP) also studied the use of ERS-1 images for the purpose of tropical vegetation monitoring, combining the use of thematic interpretation, data processing and new initiatives for large scale radar maps [63].

The use of image processing techniques together with SAR images to estimate different forest parameters were also researched. Foody *et al*. [64] proposed the use of neural networks to estimate the diversity and composition of a Bornean tropical rain forest using Landsat TM data. In the study, a feedforward neural network was applied to estimate species richness while a Kohonen neural network was used to provide information on species composition. Another study focused on soil moisture estimation using a remote sensing algorithm from LANDSAT TM, ETM and ENVISAT images [65]. Preliminary results show that the empirical model used to estimate soil moisure had a poor agreement with the measured values. As such, further exploration into the model is necessary.

Tropical forest carbon stock and biomass are important parameters in forest management. Yang *et al*. [66] explored the possibility to estimate carbon stock of tropical forest vegetation using LANDSAT TM data and GIS data. A model to estimate biomass was formulated with the data of forest fixed samples, GIS and LANDSAT TM images. Finally the carbon stock was created from the biomass calculated using the above model. The model has been found to be effective. Williams *et al*. [67] proposed recovering tropical forest biomass from GeoSAR observations. The airborne GeoSAR collects X-band and P-band InSAR data simultaneously. It was shown that GeoSAR X-P interferometric data alone may be used to recover tropical forest biomass, removing any ambiguity associated with variation in ground conditions.

CONCLUSION

Remote sensing has been applied to tropical vegetation, both in agriculture and forestry. The problem of remote sensing of vegetation can be divided into three main categories: development of theoretical models, ground truth measurement techniques, and equipment and image processing.

There has been a multitude of scattering models developed to understand the interaction between tropical vegetation and electromagnetic waves. The use of Radiative Transfer theory is highly popular, though there are other theories being utilized as well. Several variations to the RT model are the multilayer model, DMPACT and Fresnel corrections, combination with the Lindenmayer System and also the Vector Radiative Transfer model. These extensions sought to improve on the accuracy of backscatter predictions and serve as the basis for the future development of inversion models.

The design and study of equipment to carry out measurements are needed to obtain ground truth data from vegetation for the purpose of model validation. There are research groups focusing on the development of ground based and airborne scatterometers and SAR. An anechoic chamber was also designed by a research team in MMU, Cyberjaya, Malaysia, while moisture sensors have also been looked into. Lastly, there is also research on image processing to improve on image classification from spaceborne and airborne images to distinguish between different vegetation types and other land areas.

There is still much work to be done on all areas in order to develop more accurate techniques for the remote sensing of tropical vegetation.

Acknowledgements – The authors would like to thank Advanced Agriecological Research Sdn Bhd (AAR), Universiti Tunku Abdul Rahman (UTAR) and the Ministry of Science, Technology and Innovation of Malaysia (MOSTI) for their support in the project.

REFERENCES

1. Chuah H.T. (1997) An Overview of Microwave Remote Sensing Research at the University of Malaya, Malaysia. *Proceedings of IEEE International Geoscience and Remote Sensing Symposium* **3**: 1421–1423.
2. Golden, K.M.; Borup, D.; Cheney, M.; Cherkaeva, E.; Dawson, M.S.; Kung-Hau Ding; Fung, A.K.; Isaacson, D.; Johnson, S.A.; Jordan, A.K.; Jin An Kon; Kwok, R.; Nghiem, S.V.; Onstott, R.G.; Sylvester, J.; Winebrenner, D.P.; Zabel, I.H.H. (1998) Inverse Electromagnetic Scattering Models for Sea Ice. *IEEE Transactions on Geoscience and Remote Sensing* **36(5)**: 1675–1704.
3. Fernandez D.E.; Chang P.S., Carswell J.R., Contreras R.F. and Frasier S.J. (2005) IWRAP: The Imaging Wind and Rain Airborne Profiler for Remote Sensing of the Ocean and the Atmospheric Boundary Layer Within Tropical Cyclones. *IEEE Transactions on Geoscience and Remote Sensing* **43(8)**: 1775–1787.
4. Guerif M., Launay M. and Duke C. (2000) Remote sensing as a tool enabling the spatial use of crop models for crop diagnosis and yield prediction. *Proceedings of IEEE International Geoscience and Remote Sensing Symposium* **4**: 1477–1479.
5. Lelong C.C.D., Roger J.-M., Bregand S., Dubertret F., Lanore M., Sitorus N.A., Raharjo D.A. and Caliman J.-P. (2009) Discrimination of Fungal Disease Infestation in Oil-Palm Canopy and *Hyperspectral Reflectance Data. Proceedings of First Workshop on Hyperspectral Image and Signal Processing: Evolution in Remote Sensing*: 1–4.
6. Sawada H., Nakakita O., Awaya Y., Hamzah K.A. and Hassan A. (1991) Development of Monitoring System for Tropical Rain Forest Management in the Peninsula Malaysia: The Joint Malaysia-Japan Research Project on Remote Sensing. *Proceedings of IEEE International Geoscience and Remote Sensing Symposium: Remote Sensing: Global Monitoring for Earth Management* **3**: 1153–1156.
7. Koay J.Y., Tan C.P., Lim K.S., Saiful Bahari A.B., Ewe H.T., Chuah H.T. and

Kong J.A. (2007) Paddy Fields as Electrically Dense Media: Theoretical Modeling and Measurement Comparisons. *IEEE Transactions on Geoscience and Remote Sensing* **45(9)**: 2837–2849.

8. Yueh S. H., Kong J. A., Jao J. K., Shin R. T. and Le Toan T. (1992) Branching Model for Vegetation," *IEEE Transactions on Geoscience and Remote Sensing* **30(2)**: 390–402.
9. Tsang L., Ding K. H., Zhang G., Hsu C. C. and Kong J. A. (1995) Backscattering Enhancement and Clustering Effects of Randomly Distributed Dielectric Cylinders Overlying a Dielectric Half Space based on Monte-Carlo Simulations. *IEEE Transactions on. Antennas and Propagation* **43(5)**: 488–499.
10. Chuah H.T, Tjuatja S., Fung A.K. and Bredow, J.W. (1996) A Phase Matrix for a Dense Discrete Random Medium: Evaluation of Volume Scattering Coefficient. *IEEE Transactions on Geoscience and Remote Sensing* **34(5)**: 1137-1143.
11. Ewe H.T. and Chuah H.T. (2000). Electromagnetic Scattering from an Electrically Dense Vegetation Medium. *IEEE Transactions on Geoscience and Remote Sensing* **38(5)**: 2093-2105.
12. Fung A. K. and Chen M. F. (1987) Fresnel Field Interaction Applied to Scattering from a Vegetation Layer. *Remote Sensing of Environment*. **23(1)**: 35–50.
13. Ewe H. T. and Chuah H. T. (2000) A Study of Fresnel Scattered Field for Nonspherical Discrete Scatterers. *Progress in Electromagnetics Research* **25**: 189–222.
14. Fung A.K. (1994) *Microwave Scattering and Emission Models and Their Applications*. Artech House, Norwood, Massachusetts.
15. Chandrasekhar S. (1960) *Radiative Transfer*. Dover, New York.
16. Ulaby F. T., Moore R. K. and Fung A. K. (1982) *Microwave Remote Sensing: Active and Passive, Vol. II*. Artech House, Norwood, Massachusetts.
17. Karam M. A., Fung A. K., Lang R. H. and Chauhan N. S. (1992) A Microwave Scattering Model for Layered Vegetation. *IEEE Transactions on Geoscience and Remote Sensing* **30(4)**: 767–784.
18. Le Toan T., Ribbes F., Wang L. F., Floury N., Ding K. H., Kong J. A., Fujita M. and Kurosu T. (1997) Rice Crop Mapping and Monitoring Using ERS-1 Data Based on Experiment and Modeling results. *IEEE Transactions on Geoscience and Remote Sensing* **35(1)**: 41–56.
19. Kurosu T., Suitz T., and Moriya T. (1995) Monitoring of Rice Crop Growth from Space using ERS-1 C-Band SAR," *IEEE Transactions on Geoscience and Remote Sensing* **33(4)**: 1092–1096.
20. Koay J.Y., Ewe H.T. and Chuah H.T. (2008) A Study of Fresnel Scattered Fields for Ellipsoidal and Elliptic-Disk-Shaped Scatterers. *IEEE Transactions on Geoscience and Remote Sensing* **46(4)**: 1091–1103.
21. Ma H.B., Zeng Q.M., Ma A.N. and Zhang T. (2000) Simulation and Analysis for the Microwave Backscattering Coefficient of Rice. *Proceedings of IEEE International Geoscience and Remote Sensing Symposium* **2**: 369–371.
22. Ulaby F.T., Sarabandi K., MacDonald K., Whitt M., and Dobson M. C. (1990) Michigan Microwave Canopy Scattering Model. *International Journal of Remote Sensing* **11**, 1223–1253.

23. Shao Y., Liao J.J, Fan X.T. and Wang Y.H. (2002) Analysis of Temporal Backscatter of Rice: A Comparison of RADARSAT Observations with Modeling Results. *Proceedings of IEEE International Geoscience and Remote Sensing Symposium: Remote Sensing* **1**: 478–480.
24. Sun G., Simonett D., and Strahler A. (1991) A Radar Backscatter Model for Discontinuous Coniferous Forests. *IEEE Transactions on Geoscience and Remote Sensing* **29(4)**: 639–650.
25. Ulaby F. T. and El-Rayes M. A. (1987) Microwave Dielectric Spectrum of Vegetation-Part II: Dual-Dispersion Model. *IEEE Transactions on Geoscience and Remote Sensing* **GE-25(5)**: 550–557.
26. Fortuny-Guasch J., Martinez-Vazquez A., Riccio D., Lopez-Sanchez J.M. and Ballester J.D. (2003) Experimental Validation of an Electromagnetic Model for Rice Crops Using a Wide-Band Polarimetric Radar. *Proceedings of IEEE International Geoscience and Remote Sensing Symposium* **4**: 2866–2868.
27. Ma H.B., Zeng Q.M., Ma A.N. (2000) Backscattering Model for Crops Based on L-system and Coherent Addition of Scattered Field. *Proceedings of IEEE International Geoscience and Remote Sensing Symposium* **2**: 907–909.
28. Lindenmayer A. (1968) Mathematical Models for Cellular Interaction in Development, I and 11. *Journal of Theoretical Biology* **18**: 280–315.
29. Liao J.J, Guo H.D. and Shao Y. (2002) Modeling of Microwave Dielectric Properties of Rice Growth Stages in Zhaoqing Test Site of Southern China. *Proceedings of IEEE International Geoscience and Remote Sensing Symposium* **5**: 2620–2622.
30. Zhang Y., Huang H., Chen X. and Wu J. (2008) Mapping Paddy Rice Biomass Using ALOS/PALSAR Imagery. *Proceedings of 2008 International Workshop on Education Technology and Training & 2008 International Workshop on Geoscience and Remote Sensing* **2**: 207–210.
31. Wang C., Wu J., Zhang Y., Qi J. and Salas W.A. (2009) Characterizing L-Band Scattering of Paddy Rice in Southeast China with Radiative Transfer Model and Multitemporal ALOS/PALSAR Imagery," *IEEE Transactions on Geoscience and Remote Sensing* **47(4)**: 988–998.
32. Durden S.L., Morrissey L.A. and Livingston G.P. (1995) Microwave Backscatter and Attenuation Dependence on Leaf Area Index for Flooded Rice Fields. *IEEE Transactions on Geoscience and Remote Sensing* **33(3)**: 807–810.
33. Inoue Y., Dabrowska-Zielinska K., Kurosu T., Maeno H., Uratsuka S. and Kozu T. (2001) Interactions between Multi-Frequency Microwave Backscatters and Rice Canopy Variables. *Proceedings of IEEE International Geoscience and Remote Sensing Symposium: Remote Sensing* **3**: 1270–1272.
34. Izzawati, Lewis P. and McMorrow J. (1998) 3D Model Simulation of Polarimetric Radar Backscatter and Texture of An Oil-Palm Plantation. *Proceedings of IEEE International Geoscience and Remote Sensing Symposium* **3**: 1502–1504.
35. Sun G. and Ranson K.J. (1995) A Three-Dimensional Radar Backscatter Model of Forest Canopies. *IEEE Transactions on Geoscience and Remote Sensing* **33(2)**: 372–382.
36. Chauhan N.S., Lang R.H. and Ranson K.J. (1991) Radar Modeling of a Boreal Forest.

IEEE Transactions on Geoscience and Remote Sensing **29(4)**: 627–638.
37. Thirion L., Colin E. and Dahon C. (2006) Capabilities of a Forest Coherent Scattering Model Applied to Radiometry, Interferometry, and Polarimetry at P- and L-Band. *IEEE Transactions on Geoscience and Remote Sensing* **44(4)**: 849–862.
38. Koo V.C., Chung B.K. and Chuah H.T. (2003) Development of a Ground-Based Radar for Scattering Measurements. *IEEE Antennas and Propagation Magazine* **45(2)**: 36–42.
39. Xu C.L, Chen Y., Tong L., Jia M.Q., Liu Z.C. and Lu H.P. (2008) Measuring the Microwave Backscattering Coefficient of Paddy Rice Using FM-CW Ground-based Scatterometer. *Proceedings of 2008 International Workshop on Education Technology and Training & 2008 International Workshop on Geoscience and Remote Sensing* **2**: 194–198.
40. Zhao C.W, Chen Y., Tong L. and Jia M.Q., (2011) Multi-frequency and Multi-polarization Radar Measurements Over Paddy Rice Field and Their Relationship with Ground Parameters. *Proceedings of IEEE International Geoscience and Remote Sensing Symposium: Remote Sensing* **3**: 1958–1960.
41. Kim S.B., Kim B.W., Kong Y.K. and Kim Y.S. (2000) Radar Backscattering Measurements of Rice Crop Using X-Band Scatterometer. *IEEE Transactions on Geoscience and Remote Sensing* **38(3)**: 1467–1471.
42. Koo V.C., Chan Y.K., Gobi V., Lim T.S., Chung B.K. and Chuah H.T. (2005) The Masar Project: Design and Development. *Progress in Electromagnetics Research* **50**: 279–298.
43. Chan Y.K., Azlindawaty M.K., Gobi V., Chung B.K. and Chuah H.T. (2000) The Design and Development of Airborne Synthetic Aperture Radar. *Proceedings of IEEE International Geoscience and Remote Sensing Symposium* **2**: 518–520.
44. Chan Y.K., Chung B.K. and Chuah H.T. (2004) Transmitter and Receiver Design of an Experimental Airborne Synthetic Aperture Radar Sensor. *Progress in Electromagnetics Research* **49**: 203–218.
45. Chung B.K. and Chuah H.T. (2003) Design and Construction of a Multipurpose Wideband Anechoic Chamber. *IEEE Antennas and Propagation Magazine* **45(6)**: 41–47.
46. Chung B.K., Teh C.H. and Chuah H.T. (2004) Modeling of Anechoic Chamber Using a Beam-tracing Technique. *Progress in Electromagnetics Research* **49**: 23–38.
47. Chung B.K. and Chuah H.T. (2003) Modeling of RF Absorber for Application in the Design of Anechoic Chamber. *Progress in Electromagnetics Research* **43**: 273–285.
48. Chung B.K., Chuah H.T. and Bredow J.W. (1997) A Microwave Anechoic Chamber for Radar-Cross Section Measurement. *IEEE Antennas and Propagation Magazine* **39(3)**: 21–26.
49. Khalid K., Ghretli, M.M., Abbas Z. and Grozescu I.V. (2006) Development of Planar Microwave Moisture Sensors for Hevea RubberLatex and Oil Palm Fruits. *Proceedings of International RF and Microwave Conference*: 10–15.
50. Chuah H.T., Lee K.Y. and Lau T.W. (1995) Dielectric Constants of Rubber and

Oil Palm Leaf Samples at X-Band. *IEEE Transactions on Geoscience and Remote Sensing* **33(1)**: 221–223.
51. Fung A.K. and Fung H.S. (1977) Application of First-Order Renormalization Method to Scattering from a Vegetation-Like Half-Space. *IEEE Transactions on Geoscience Electronics* **15(4)**: 189–195.
52. Ulaby F.T. and El-Rayes M.A., (1987) Microwave Dielectric Spectrum of Vegetation-Part 2: Dual-Dispersion Model," *IEEE Transactions on Geoscience and Remote Sensing* **25(5)**: 541–549.
53. Rees A.R. and Tinker P.B.H. (1963) Dry-Matter Production and Nutrient Content of Plantation Oil Palms in Nigeria. *Plant and Soil* **16(3)**: 350–363.
54. Asari N., Suratman M.N. and Jaafar J. (2011) Preliminary Study of Above Ground Biomass (AGB) and Stem Volume of Oil Palm Stands. *Proceedings of IEEE Symposium on Business, Engineering and Industrial Applications*: 65–70.
55. Kim Y.Y., Jackson T., Bindlish R., Lee H.Y. and Hong S.Y. (2012) Radar Vegetation Index for Estimating the Vegetation Water Content of Rice and Soybean. *IEEE Geoscience and Remote Sensing Letters* **9(4)**: 564–568.
56. Suitz, T., Kurosu, T. and Umehara, T. (1988) A Measurement Of Microwave Backscattering Coefficients Of Rice Plants. *Proceedings of IEEE International Geoscience and Remote Sensing Symposium* **3**: 1283–1286.
57. Yang C.J., Zhou J.M., Huang H. and Chen X. (2007) Correlations of the Biomass of the Main Topical Forest Vegetation Types and LANDSAT TM Data in Xishuangbanna of P. R. of China. *Proceedings of IEEE International Geoscience and Remote Sensing Symposium*: 4336–4338.
58. Ouchi K. and Ipor I.B. (2002) Comparison of SAR and Optical Images of the Rainforests of Borneo, Malaysia with Field Data. *Proceedings of IEEE International Geoscience and Remote Sensing* Symposium **5**: 2905–2907.
59. Zhao X.Y, Yang S.B., Shen S.H. and Li B.B. (2011) Assessment of ENVISAT ASAR Data for Rice Monitoring Based on Three Years Experiments. *Proceedings of IEEE International Conference on Remote Sensing, Environment and Transportation Engineering*: 136–139.
60. Yamada Y. (2003) Relation between Ground Features and Mathematical Morphology Using JERS-1/SAR Data During Flooding Time in Paddy Areas. *Proceedings of IEEE International Geoscience and Remote Sensing Symposium* **4**: 2526–2528.
61. Paudyal D.R., Eiumnoh A. and Aschbacher J. (1995) Multitemporal Analysis of SAR Images Over the Tropics for Agricultural Applications. *Proceedings of IEEE International Geoscience and Remote Sensing Symposium* **2**: 1219–1221.
62. Hung L.Q. and Batelaan O. (2003) Environmental Geological Remote Sensing and GIS Analysis of Tropical Karst Areas in Vietnam. *Proceedings of IEEE International Geoscience and Remote Sensing Symposium* **4**: 2964–2966.
63. Malingreau J.P., De Grandi G.F., Leysen M., Mayaux P. and Simard M. (1997) The ERS-1 Central Africa Mosaic: A New Role for Radar Remote Sensing in Global Studies of the Tropical Ecosystem. *Proceedings of IEEE International Geoscience and Remote Sensing Symposium* **4**: 1725–1727.

64. Foody G.A. and Cutler M.E. (2002) Remote Sensing of Biodiversity: Using Neural Networks to Estimate the Diversity and Composition of a Bornean Tropical Rainforest from Landsat TM Data. *Proceedings of IEEE International Geoscience and Remote Sensing Symposium* **1**: 497–499.
65. Marrufo L., Gonzalez F., Monsivais-Huertero A. And Ramos J. (2011) Spatio-Temporal Estimation of Soil Moisture in a Tropical Region using a Remote Sensing Algorithm. *Proceedings of IEEE International Geoscience and Remote Sensing Symposium*: 3089–3092.
66. Yang C.J., Liu J.Y., Zhang Z.X. and Zhang Z.K. (2001) Estimation of the Carbon Stock of Tropical Forest Vegetation by Using Remote Sensing and GIS. *Proceedings of IEEE International Geoscience and Remote Sensing Symposium* **4**: 1672–1674.
67. Williams M.L., Milne T., Tapley I., Reis J.J., Sanford M., Kofman B. and Hensley S. (2009) Tropical Forest Biomass Recovery Using GeoSAR Observations. *Proceedings of IEEE International Geoscience and Remote Sensing Symposium* **4**: 173–176.

Lakes of Malaysia

ISBN 978-983-9445-93-0
Publisher: Academy of Sciences Malaysia, 2013
902-4 Jalan Tun Ismail, 50480 Kuala Lumpur, Malaysia; www.akademisains.gov.my.

Lakes of Malaysia is a coffee table book jointly produced by the Academy of Sciences, the National Hydraulic Research Institute Malaysia and the Department of Irrigation and Drainage Malaysia, with Academician Tan Sri Ir Shahrizaila Abdullah as Chairman of the Publication Committee. It presents a pictorial record of Malaysia's scenic natural lakes and man-made reservoirs, and showcases a range of picturesque landscapes as well as highlights the country's lakes as important natural assets to be sustainably used or developed.

This pictorial tome takes the reader on a panoramic journey across the states of Peninsular Malaysia, Sabah and Sarawak to many of the lake and reservoir sites while providing useful touristic information regarding the locations including myths and legends that surround some of the lakes.

The publication is aimed at expressing a deep appreciation of the water bodies and at creating an awareness of the need to preserve and conserve these invaluable assets. It provides an overview of the lake environment, how various natural lakes are formed and classified, biodiversity of the lake ecosystem, the many indigenous peoples that live around the lake environment, the multiple use and huge economic benefits derived from lakes and reservoirs, and innovative and eco-friendly conservation and remediation measues.

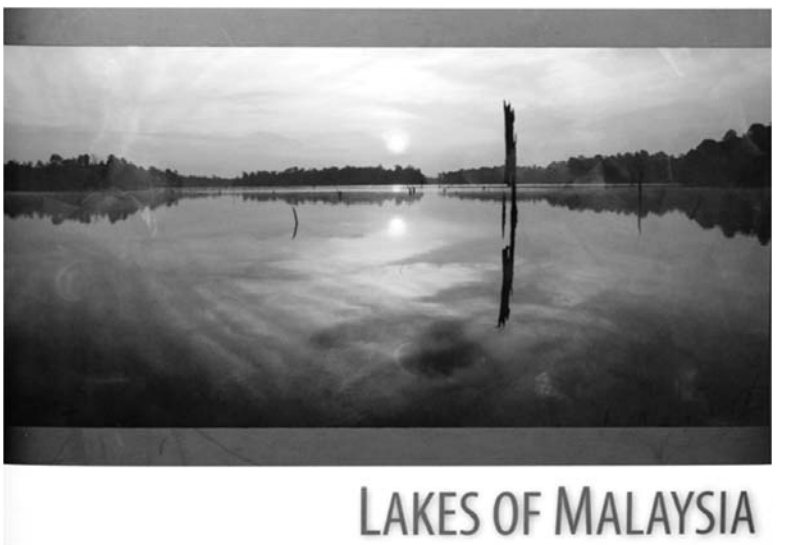

Journal of Science and Technology in the Tropics (2013) 9: 80

Biodiversity Pulau Tioman

by Yong Hoi Sen, Hj. Mohd Nawayai, Tan Poai Ean and Daicus Belabut
ISBN 978-967-5557-12-5
Publisher: Department of Wildlife and National Parks, Malaysia, 2012

Pulau Tioman (Tioman Island) is one of the most famous islands in Malaysia and an international tourist attraction. It is the largest in a group of 64 volcanic islands in the South China Sea. It has a unique geological history, rock types and landscape. Although small in land area, it has a relatively rich and diverse fauna and flora, as well as geological features.

This pictorial book provides glimpses of the biological diversity of Pulau Tioman, off the east coast of Pahang Darul Makmur, Peninsular Malaysia. It covers ecosystem diversity, plant diversity, animal diversity, and conservation. Different life forms and habits as well as the landscapes are presented to provide an overview of the great diversity of the island.

Biodiversity Pulau Tioman should be an interesting read to a variety of people from different walks of life and from different lands. The colour illustrations will help readers to appreciate the fascinating biodiversity of the island.

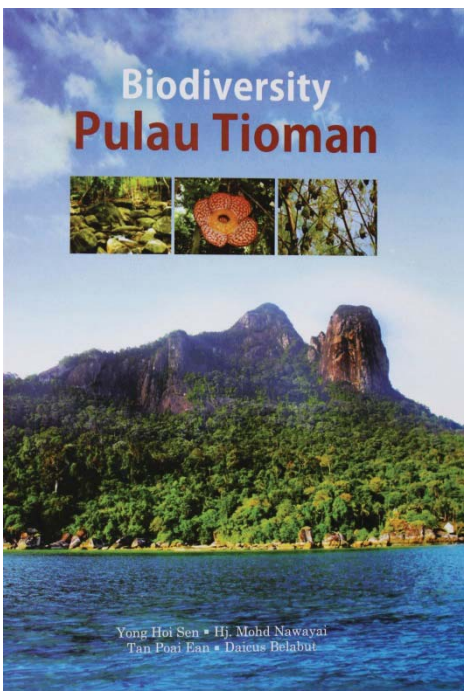

For further information about this publication, contact:
Department of Wildlife and National Parks, Malaysia, Km 10 Jalan Cheras, 56100 Kuala Lumpur, Malaysia;
www.wildlife.gov.my